1963

A nuclear magnetic resonance investigation of intermetallic compounds of yttrium with iron group metals

Stanley Lewis Segel
Iowa State University

A NUCLEAR MAGNETIC RESONANCE INVESTIGATION OF INTERMETALLIC COMPOUNDS OF YTTRIUM WITH IRON GROUP METALS

by

Stanley Lewis Segel

A Dissertation Submitted to the
Graduate Faculty in Partial Fulfillment of
The Requirements for the Degree of
DOCTOR OF PHILOSOPHY

Major Subjects: Physics
Metallurgy

Approved:

Signature was redacted for privacy.

In Charge of Major Work

Signature was redacted for privacy.

Heads of Major Departments

Signature was redacted for privacy.

Dean of Graduate College

Iowa State University
Of Science and Technology
Ames, Iowa

1963

TABLE OF CONTENTS

	Page
INTRODUCTION	1
THEORY	3
Knight Shift Interaction	3
Anisotropic Knight Shift and Nuclear Quadrupole Interaction	7
EXPERIMENTAL APPARATUS AND PROCEDURE	16
EXPERIMENTAL RESULTS AND DISCUSSION	20
Yttrium Resonances in Yttrium Metal	20
Yttrium Resonances in Scandium-Yttrium System	20
Yttrium Resonances in Yttrium-Copper System	22
Copper Resonances in Yttrium-Copper System	25
Yttrium Resonances in Yttrium-Nickel System	26
Yttrium Resonance in YMn_2	29
Scandium Resonances in Scandium Metal and Scandium-Yttrium Alloys	31
Manganese Resonances in YMn_2	44
SUMMARY	50
LITERATURE CITED	53
ACKNOWLEDGEMENTS	58
APPENDIX	59

INTRODUCTION

Electrons occupying states close to the Fermi surface are of great importance in the study of metals. This importance derives from the pairing imposed on lower energy electrons by the Pauli exclusion principle and the resultant cancellation of effects due to these lower energy electrons. The electronic contribution to the specific heat, the Pauli susceptibility and the Knight shift are phenomena due to electrons in states close to the Fermi surface.

Specifically, the Knight shift refers to the shift in frequency for the nuclear spin resonance condition of a given metallic nucleus in a metal from that at which it occurs in the metal ion. The Knight shift is described as the interaction of the nuclear magnetic moment of the metal nucleus with the spins of the conduction electrons through the hyperfine coupling. This interaction is responsible for the shift of the resonance condition and is proportional to the absolute square of the conduction electron wave function at the nuclear site averaged over the Fermi surface. Hence, observation of the Knight shift provides a sensitive test of proposed electronic wave functions. However, since the interaction involves the product of quantities which are difficult to determine from independent experiments, one is usually concerned with the variation of the Knight shift.

The observation of the Knight shift of a given nucleus across a given binary system allows one to draw some conclusions about the nature of the electron-nuclear spin interaction. This type of observation and analysis has been performed on the systems yttrium-copper, yttrium-nickel and yttrium-scandium. In addition the yttrium (89) nuclear magnetic resonance has been observed in the phase YMn_2.

Nuclei with nuclear spin greater than or equal to unity may possess quadrupole moments. The nuclear electric quadrupole moment is essentially a measure of the non-spherical nature of the nucleus. The interaction of the quadrupole moment with electric field gradients within the sample modify the magnetic energy levels and complicate the Knight shift analysis. Recent works have simplified the analysis of the resonance spectrum resulting from quadrupole interactions and the Knight shift of scandium (45), spin 7/2, in the yttrium-scandium system and the Knight shift of manganese (55), spin 5/2, in YMn_2 have been determined.

THEORY

Knight Shift Interaction

The nuclear magnetic resonance experiment consists of an absorption of radio frequency energy by the nucleus of an atom situated in a magnetic field. For a nucleus with nuclear spin I, there are $2I + 1$ equally spaced energy levels in a magnetic field. The frequency at which transitions between these energy levels takes place is given by

$$\nu = \frac{\mu H}{Ih} = (\gamma/2\pi)H \quad , \tag{1}$$

where μ is the nuclear magnetic dipole moment, Ih is the nuclear angular momentum, H is the magnetic field at the nucleus, and γ is the gyromagnetic ratio. The gyromagnetic ratio is the ratio of the nuclear dipole moment to the nuclear angular momentum.

Knight (29) first observed that the frequency associated with copper in copper wire was higher by a quarter of a percent than the respective frequency for nonmetallic copper (CuCl) in the same external field. Subsequently, Townes (48) proposed a theory which established reasonable agreement between the theoretical predictions and experimental results for copper and several other metals in which the same phenomena were observed.

The theoretical description of the situation goes as

follows. Upon application of a magnetic field, the conduction electrons become polarized and assume a magnetic moment. Since the only available energy states for the electrons are near the Fermi surface, only the electrons at the Fermi surface participate in this polarization process. The effective magnetic moment assumed by the conduction electrons is then given by

$$\mu_{eff} = \chi_p MH \quad , \tag{2}$$

where χ_p is the Pauli susceptibility per unit mass, H is the applied magnetic field, and M is the atomic mass. Those conduction electrons which are of s character have a finite probability at the nuclear position. It is via the wave functions of these conduction electrons that "touch" the nucleus that the effective magnetic moment of the conduction electrons provides a small additional magnetic field at the nuclear site. The shift in resonance condition due to this small additional field is known as the Knight shift.

The exact expression for the Knight shift is

$$\Delta\nu/\nu = \frac{8\pi}{3} \chi_p M \left\langle |\psi_F(0)|^2 \right\rangle_{AVE} \quad , \tag{3}$$

where $\left\langle |\psi_F(0)|^2 \right\rangle$ is the probability density at the nucleus of the electron wave functions determined by taking a suitable average over the electrons having energies near the Fermi

energy. It should be noted that the relationship

$$\Delta\nu/\nu = \Delta H/H \qquad (4)$$

is valid only for small values of the ratio. $\Delta\nu/\nu$ is exact, and for large shifts, $\Delta H/H$ involves higher orders of the ratio. Except for the case of the results for manganese (55) in YMn_2, Equation 4 is valid within experimental error. Several excellent reviews elaborating on the derivation of the Knight shift are given by Rowland (46) and Knight (28).

Direct evaluation of χ_p has been performed only for beryllium and the alkali metals. An indirect evaluation of χ_p is via the low temperature specific heat which is connected to the Pauli susceptibility by way of the density of states, $N(E_F)$. The susceptibility for free electrons, assuming a Fermi distribution, is

$$\chi_p = \mu_B^2 N(E_F) \quad , \qquad (5)$$

where μ_B is the Bohr magneton. The electronic heat capacity per unit mass of a metal is given by

$$C_V = \gamma T \quad , \qquad (6)$$

where $\gamma = \pi^2 k^3 N(E_F)/3$, k is Boltzman's constant and T is the absolute temperature. It is also possible to derive a value of χ_p from the measured bulk magnetic susceptibility. The

errors involved in this process may be very large and it is used as a last resort in estimating χ_P.

The quantity $\left\langle |\psi_F(0)|^2 \right\rangle_{AVE}$, sometimes called P_F, is equally difficult to determine. Kohn (32) has described a difficult method of calculating it directly. It may also be evaluated from the hyperfine constants with an equal amount of difficulty.

The Knight shift is independent of temperature unless χ_P or P_F depends on temperature. These quantities are expected to exhibit a temperature dependence only indirectly because of thermal expansion. The density of states per unit mass which appears in Equation 5 should vary as $(\text{volume})^{2/3}$ in a free electron approximation and such a dependence has been observed in the case of sodium as shown by McGarvey (36) and Knight (30). The change in P_F due to a volume change is estimated theoretically to be very small.

The measurement of ΔH may be uncertain by the magnitude of the variation of the chemical shifts among the non-metallic compounds of the same element. One means by ΔH the difference between the magnetic field which would prevail at the nucleus if the spins of the conduction electrons were all paired and the magnetic field which actually exists in the real metal assuming the externally applied field to be a constant. However, this approximation may be quite poor under certain conditions: if the molecules of the reference compound

populate paramagnetic excited states; if the atom cores are distorted differently in the various chemical compounds or in the metallic lattices; if the diamagnetic effects of the valence electrons depend somewhat on the molecular bonding. This is discussed by Knight (28). A further complication arises from the fact that the chemical shifts for solutions sometimes depend on concentration.

Anisotropic Knight Shift and Nuclear Quadrupole Interaction

The presence of anisotropy in the Knight shift and nuclear electric quadrupole interactions have the effect of both shifting the resonance position and broadening the resonance asymmetry and thus make an evaluation of the Knight shift more difficult. Discussions of the anisotropy of the Knight shift and of quadrupole effects have been given by Bloembergen (7) and Cohen (12). It will suffice here to describe the interactions, their effect on the magnetic or central transition ($m = +1/2 \longleftrightarrow m = -1/2$), and the method which enables one to extract the Knight shift parameter.

Bloembergen (7) has demonstrated that the effects of anisotropy in the distribution of electron charge density cause characteristic changes in the shape of the nuclear resonance observed using the customary powdered metal samples. Actually, each crystallite in the agglomerate would, if its

resonance could be viewed alone, show a symmetric resonance whose position would depend on the orientation of the crystal axes with respect to the external magnetic field. The resonance would move within a small frequency region as the crystallite orientation was changed, the extreme position of the line corresponding to alignment of the symmetry axis of the lattice parallel or perpendicular to the external magnetic field. In experiments on powders, essentially all orientations are represented and absorption of energy takes place over the whole range of frequencies producing a line which is much like an absorption line except humped on one side.

It should be noted that the identical effect could be obtained from an anisotropy of the g value of the conduction electrons. The combined effect would be inseparable and it is usually discussed in terms of the anisotropic shift charge distribution.

The total shift is due to the sum of the fields at the nucleus; ΔH_{iso}, the previously discussed isotropic, orientation independent contribution and ΔH_{aniso}, sometimes called ΔH_{ax}, the orientation dependent part produced by the anisotropy in the charge distribution described by the non-s wave functions.

Bloembergen (7) gives

$$\frac{\Delta\nu}{\nu} = \frac{\Delta H}{H} = \mu_B{}^2 \Omega N(E_F) q_F (3\cos^2\theta - 1) \quad , \qquad (7)$$

where

$$q_F = \left\langle \int \psi^*(3z^2 - r^2)r^{-3}\psi dV \right\rangle \qquad (8)$$

and is a measure of the anisotropy in the charge distribution. ψ and ψ^* are wave functions with the property that $\psi\psi^*$ represents the average electron density in space of the conduction electrons near the Fermi level. The integral in Equation 8 is over the unit atomic cell and the average is over the Fermi surface. The angle θ is the angle between the symmetry axis of the crystal, designated the z axis, and the external magnetic field direction. It is common to let $\mu_B{}^2\Omega N(E_F)q_F = K_{ax}$, then called the anisotropic Knight shift.

Further, from Bloembergen (7)

$$\Delta\nu = \Delta\nu_{\parallel} \cos^2\theta + \Delta\nu_{\perp} \sin^2\theta \qquad (9)$$

or $$\nu - \nu_R = (\nu_{\parallel} - \nu_R) \cos^2\theta + (\nu_{\perp} - \nu_R) \sin^2\theta \quad ,(10)$$

where ν_R is the frequency of the reference for the given applied field. Then

$$\nu = \nu_{\parallel} \cos^2\theta + \nu_{\perp} \sin^2\theta \quad , \qquad (11)$$

where

$$\begin{aligned} \nu &= \nu_{iso} + 2 K_{ax} \nu_R \\ &= \nu_R(1 + K_{iso}) + 2 K_{ax} \nu_R \end{aligned} \qquad (12)$$

$$\text{and} \quad \nu = \nu_{iso} - K_{ax}\,\nu_R = \nu_R(1 + K_{iso}) - K_{ax}\,\nu_R \quad . \tag{13}$$

Finally,

$$\nu = \nu_{iso}\left[1 + \frac{K_{ax}}{1 + K_{iso}}\,(3\cos^2\theta - 1)\right] \quad . \tag{14}$$

The averaging procedure for polycrystalline samples is given by Pake (40) and yields an intensity maximum at $\theta = 90^{o}$ and the frequency at this angle will be then

$$\nu^{II} = \nu_{iso}(1 - a) \quad , \tag{15}$$

where

$$a = \frac{K_{ax}}{1 + K_{iso}} \quad .$$

A discontinuity or step also occurs at $\theta = 0^{o}$ and the frequency at this angle will be then

$$\nu^{I} = \nu_{iso}(1 + 2a) \quad . \tag{16}$$

The apparent line width or "splitting" will then be

$$\nu^{I} - \nu^{II} = \nu_{iso} + 2a\nu_{iso} - \nu_{iso} + a\nu_{iso} \quad , \tag{17}$$

$$\Delta\nu = 3a\nu_{iso} \quad . \tag{18}$$

The line shape of a nuclear magnetic resonance in the

case of anisotropic Knight shift only is characterized by a width which is proportional to the resonance frequency or field and an asymmetric appearance which provides an indication of the sign of the axial component of the shift.

The effect of a weak nuclear electric quadrupole interaction on the nuclear Zeeman levels has been given by Cohen (12). Because of the particular orientation dependence which the central transition acquires in second-order perturbation theory, Pound (42), the averaged expression for it possesses two maxima. These correspond to $\theta = 90^{\circ}$ and $\cos^2\theta = 5/9$ and the frequencies at which these maxima occur are given respectively by Equations 19 and 20.

$$\nu^{III}\ (m = 1/2 \longleftrightarrow m = -1/2) = \nu_R + \frac{\nu_Q^2}{16\nu_R}\,[I(I+1) - 3/4]\ , \tag{19}$$

$$\nu^{IV}\ (m = 1/2 \longleftrightarrow m = -1/2) = \nu_R - \frac{\nu_Q^2}{9\nu_R}\,[I(I+1) - 3/4]\ , \tag{20}$$

where $\nu_Q = e^2qQ/2I(2I-1)h$, q is the electric field gradient, Q is the quadrupole moment of the nucleus with nuclear spin I, and ν_R is the frequency of the resonance condition in the absence of quadrupole interaction. This

brief discussion excludes Knight shift effects. Neglecting other broadening mechanisms, the apparent line width is given by

$$\nu^{III} - \nu^{IV} = \frac{25\,\nu_Q^2}{144\,\nu_R}\,[I(I+1) - 3/4] \quad . \qquad (21)$$

As a check we see that when the quadrupole interaction is zero, implying either $q = 0$ or $Q = 0$, the line width is zero. This continues to neglect other broadening mechanisms such as nuclear dipolar broadening.

The line shape of a nuclear magnetic resonance in the case of nuclear electric quadrupole interaction only is characterized by a line width which is inversely proportional to the resonance frequency or field and a shifting of the resonance center of gravity to higher frequencies at constant field.

The combined effect of nuclear electric quadrupole interaction, isotropic Knight shift, and anisotropic Knight shift has been discussed by Jones (26). Qualitatively the combined effects provide three angular positions at which maxima in the intensity appear. These are $\cos\theta = 0$, $\cos^2\theta = 5/9$, and $\cos\theta = 1$. Each of these has corresponding to it a frequency given by the following equations:

$$\nu_H = \nu(\cos\theta = 0) = \nu_{iso} + b/\nu_{iso} - a\nu_{iso} \quad , \qquad (22)$$

$$\nu_L = \nu(\cos^2\theta = 5/9)$$

$$= \nu_{iso} - \frac{16b}{9a\,\nu_{iso}} + \frac{2a\,\nu_{iso}}{3} - \frac{a^2\,\nu_{iso}^3}{4b} \quad , \tag{23}$$

$$\nu = \nu(\cos\theta = 1) = \nu_{iso} + 2a\,\nu_{iso} \quad , \tag{24}$$

where again $\nu_{iso} = \nu(1 + K_{iso})$, $b = \nu_Q^2\,[I(I+1) - 3/4]/16$ and one means by ν_H the high frequency intensity maximum, by ν_L the low frequency intensity maximum and by ν_S the frequency of the discontinuity or step.

It is possible for these intensity maxima to cross each other depending on the values of the parameters a, b, and ν_{iso}. It is this point which provides the main difficulty of interpretation. Jones (26) discusses this situation in great detail. The results of basic interest for the purposes of this research are the apparent widths of the resonances and the definition for purposes of analysis of the quantities K_H and K_L.

From Equations 22, 23, and 24 we obtain the following:

$$\nu_H - \nu_S = \Delta\nu_{HS} = b/\nu_{iso} - 3a\,\nu_{iso} \quad ,$$

$$\nu_{iso}^2 < b/3a \quad ,$$

$$= 3a\,\nu_{iso} - b/\nu_{iso} \quad , \tag{25}$$

$$\nu_{iso}^2 > b/3a;$$

$$\nu_H - \nu_L = \Delta\nu_{HL} = \frac{25b}{9\,\nu_{iso}} - \frac{5a\,\nu_{iso}}{3} + \frac{a^2\,\nu_{iso}^3}{4b} \quad , \tag{26}$$

$$a > 0, \quad \frac{8b}{3a} \leq \nu_{iso}^2 \quad ;$$

$$\nu_S - \nu_L = \Delta\nu_{SL} = \frac{16b}{9\,\nu_{iso}} + \frac{4a\,\nu_{iso}}{3} + \frac{a^2\,\nu_{iso}^3}{4b} \quad , \tag{27}$$

$$a < 0, \quad \nu_{iso} \leq \frac{8b}{3a} \quad ;$$

$$K_H = \frac{\nu_H - \nu_R}{\nu_R} = K_{iso} - a + b/\nu \quad ; \tag{28}$$

$$K_L = \frac{\nu_L - \nu_R}{\nu_R} = K_{iso} + \frac{2a}{3} + \frac{16\,b}{9\,\nu_R^2} + \frac{a^2\,\nu_R^2}{4b} \quad . \tag{29}$$

Equations 25, 26, and 27 are useful in that if $\nu\Delta\nu$ vs. ν^2 is plotted, the intercept is a measure of the quadrupole coupling and the slope is a measure of the anisotropy. Equations 28 and 29 are useful in that if K_H or K_L vs. $\frac{1}{\nu_R^2}$ is plotted, the slope is a measure of the quadrupole coupling and the intercept is a measure of K_{iso} and a. This neglects the $\frac{a^2\,\nu_R^2}{4b}$ term in K_L. It is convenient at times to substitute ν_o for ν_{iso} to avoid the long subscript notation.

Discussion of the "satellite" behavior has been avoided thus far to avoid confusion with the central resonance. Pound (42) and Cohen (12) discuss this in detail for weak

interactions. The quadrupole interaction removes the degeneracy of the 2I transition frequencies such that we observe 2I-1 resonances other than the central resonance. The m $\longrightarrow$ m-1 state transition has an intensity maximum at cos θ = 0 in a powder sample and the transition frequency, based on 2nd order perturbation theory, is given by

$$\nu(m \longrightarrow m-1) = \nu_o - \frac{\nu_Q(2m-1)}{4} - \frac{\nu_Q^2}{16\nu_o}[3m(m-1) - I(I+1) + 3/2] \tag{30}$$

$$= \nu_o \{1 - [a + 1/2 \frac{\nu_Q}{\nu_o}(m - 1/2)]\} \quad .$$

The frequency difference between corresponding satellites is seen to be independent of both the isotropic and anisotropic Knight shifts and provides an unambiguous determination of the coupling constant, provided that 3rd and higher order perturbation contributions are negligible. One means by "corresponding satellites" transitions with final and initial states differing only in sign. For example, $\nu(+3/2 \longleftrightarrow + 1/2)$ and $\nu(-1/2 \longleftrightarrow - 3/2)$ are corresponding satellite transitions.

EXPERIMENTAL APPARATUS AND PROCEDURE

The nuclear magnetic resonance experiments were performed on a Varian Associates wide line NMR Spectrometer, model V-4200B. This spectrometer is an induction spectrometer described by Bloch (6). He obtained expressions for the total magnetic susceptibility $\chi = \chi' + i\chi''$, where χ' is the real part of the susceptibility and χ'' is the imaginary part. Either component of the susceptibility can be detected by properly adjusting the equipment. χ'' produces a magnetization which is out of phase with the radio-frequency field inducing the transitions and can thus be shown to be entirely responsible for the absorption of energy by the nuclear spin system. The real component of the susceptibility, χ', is responsible for the component of the nuclear magnetization in phase with the radio-frequency field and describes the dispersion accompanying the absorption. In the nuclear induction method, these components of magnetization are observed directly by the voltage they induce into a receiving coil which is placed with its axis perpendicular to the plane containing the static magnetic field and the radio-frequency field H_1.

At equilibrium, with H_1 equal to zero, the population of the nuclear spin energy levels assumes a Boltzman distribution. As H_1 is increased the energy of the spin system rises. If relaxation mechanisms, by means of which the spin system

can lose energy to the lattice, are insufficient the energy levels tend to become equally populated. As this happens the resonance intensity diminishes to zero and the signal is said to be saturated. Redfield (43) has shown that the absorption signal saturates at smaller H_1 than the dispersion signal.

The best line width measurements are made with absorption mode signals and in many cases this signal is difficult to obtain. For instance, the absorption mode signal in yttrium metal is not observable at any value of H_1. The dispersion mode signal displays the correct resonance position for symmetric resonances but provides no easy means of determining the line width.

In the work to be described a saturated solution of $Y(NO_3)_3$ was used as an yttrium (89) reference, a saturated solution of $Sc(NO_3)_3$ as a scandium (45) reference, and a saturated $NaMnO_4$ solution for a manganese (55) reference.

To measure a Knight shift one places the sample in the spectrometer and records the resonance. The resonance is recorded at constant frequency with magnetic field scanning unit providing a variation in field. One then removes the sample and substitutes the reference sample. This is then recorded. By determining the distance between the two resonances one has an estimate of the Knight shift. This distance is usually measured in terms of dial units on the

scanning unit. It is then necessary to calibrate the scanning unit to determine the number of gauss which correspond to a given number of dial units. In the case of Knight shifts of the order of 0.2% or more, it is sufficient to calibrate the scanning unit in an absolute sense; that is, determine what magnetic field corresponds to a given dial setting. For a given frequency of operation, the reference occurs at a known magnetic field. One then simply determines the difference between the metal sample resonance field position and the known reference field position. This method depends on a stable frequency source and a reproducible scan. By cycling the magnet across the field scan some ten to fifteen times, a given scanning position will reproduce itself to within 0.1 - 0.2 gauss. Since the magnetic shifts that one measures for large Knight shifts are of the order of 20 gauss, this represents an error of 1%.

Knight shifts are measured at 77 ^{o}K by placing the sample in a liquid nitrogen glass dewar which has an unsilvered tip which can be fitted into the spectrometer. This necessitates the use of narrower sample tubes and a resultant reduction in sample volume which at times adversely affects the intensity of the resonance.

Temperatures between room temperature and 77 ^{o}K are obtained by placing the sample in a dewar pipe which is placed in the spectrometer and by blowing cold, dry nitrogen

gas through the pipe. A copper-constantan thermocouple, imbedded in the sample, indicates the temperature.

The magnetic susceptibilities were measured on a Gouy apparatus whose design is described elsewhere (Hansen (22)). The temperature dependence of the susceptibility was measured for those samples where a significant variation occurred between room temperature and 77 ^{o}K.

EXPERIMENTAL RESULTS AND DISCUSSION

Yttrium Resonances in Yttrium Metal

The yttrium (89) resonance in ytterium metal was first observed by Jones (25) on a sample of yttrium metal of better than 99.9% purity which had been filed to a particle size less than the skin depth of 280 microns. This same sample was used in the present investigation. The room temperature Knight shift of 0.321% indicated in Table 1 differs from Jones (25) because of the use of a different reference compound. Jones (25) used a saturated YCl_3 solution while this research used a saturated $Y(NO_3)_3$ solution as reference.

The Knight shift at 77 ^{o}K was found to be 0.300%. Meyerhoff (37) has calculated the temperature dependence of the atomic volume of yttrium and this is insufficient to account for the temperature dependence of the Knight shift.

The yttrium (89) resonance was observable using dispersion mode signal only and any anisotropy in the shift is unknown.

Yttrium Resonances in Scandium-Yttrium System

Yttrium and scandium are hexagonal close packed metal which combine to form a random hexagonal close packed solid solution at all concentrations. This system has been

studied by Beaudry and Daane (3) whose samples were used for this investigation. The impurity content of the metals used to prepare the samples is given in Table 2.

Specimens of several compositions were filed, and the filings were sieved through a 200 mesh screen and annealed in vacuo at 500 °C for a minimum of twelve hours. The experimentally observed yttrium (89) Knight shifts, K_Y, in the yttrium-scandium solid solutions are given in Table 3 and plotted in Figure 1. No measurement on the 50.0% Y-Sc alloy sample at 77 °K was possible because of a poor signal to noise ratio.

It is observed that the K_Y at 77 °K is lower than the room temperature K_Y for all alloy compositions as well as for pure yttrium. The possibility that "core polarization" is the mechanism for this will be discussed in connection with the yttrium resonance in YMn_2. Complicating our understanding is the fact that the temperature dependence of K_Y in yttrium metal is opposite to the temperature dependence observed for the lanthanum (139) Knight shift and the scandium (45) Knight shift as shown by Blumberg (8). Yet all three metals have a hexagonal crystal structure and an identical outer electron configuration.

The approximately linear dependence of the Knight shift on concentration in other alloy systems, as was found for yttrium in these alloys, has been observed by Drain (16)

and Webb (50). As will be seen later in the discussion of the scandium (45) Knight shifts, it is possible to deduce the density of states from Knight shifts of both.

Yttrium Resonances in Yttrium-Copper System

The yttrium-copper and yttrium-nickel systems differ markedly from the yttrium-scandium system. The latter is characterized by continuous solid solubility and the former by formation of a large number of phases, each with a limited range of composition. The formation of phases of different crystal structure impedes the interpretation of the variation of the Knight shift. One usually associates the variation of the Knight shift directly with the variation of the density of states in the conduction band, particularly if other interactions can be neglected. But this can only be done if the crystal structure remains the same. One of the reasons for the formation of phases with different crystal structure across a given system is to somehow accomodate the increasing (or decreasing) electron/atom ratio to the density of states. In analogy, if we hold the electron/atom ratio constant and somehow change the crystal structure, the density of states and the Fermi energy will change in value.

The yttrium-copper system has been studied by Domagala (15) and Beaudry (3). The samples used in this investigation were those prepared by Beaudry (3). Buttons of the phases to

be studied were filed and sieved through a 200 mesh screen. Those phases which had a non-cubic crystal structure were annealed at 550 °C in vacuo but the results after annealing were identical to those before annealing. The experimental results for the yttrium (89) Knight shifts and the paramagnetic susceptibility are given in Table 1. The electron/atom ratio is determined on the basis of the assumption that copper contributes one electron to the conduction band and that yttrium contributes three electrons.

The exact number of phases formed in the yttrium-copper system is still unknown. In particular, the existence of YCu_3 and YCu_5 are still in doubt. Further, the nuclear resonance experiment does not contribute any definitive arguments concerning the matter.

In studying the phase YCu_3, the nuclear resonance experiment "straddled" this particular composition; that is, an yttrium resonance was observed in YCu_2 but no yttrium resonance was observed in YCu_4. Conversely, a copper resonance was observed in YCu_4 but not in YCu_2. It was thought then that there would be no confusion of the resonances of one phase with another. In an alloy with the stoichiometry of YCu_3 one yttrium resonance was observed with a Knight shift similar to that of the yttrium resonance in YCu_2. Also, a copper resonance was found with a Knight shift similar to that of copper in YCu_4. Yet, metallographic

examination failed to indicate the existence of two phases in the alloy YCu_3. It should be noted that the nuclear resonance experiments are not definitive and that the resonances observed may correspond to the true values in the real phase YCu_3.

In much the same way, the existence of the phase YCu_5 is tentative. The Knight shifts in YCu_5 are different from the shifts in adjacent phases beyond the experimental error. Beaudry (3) has indicated that there is some evidence from thermal data for a solubility range for YCu_6 which might extend sufficiently far to cover the stoichiometry of YCu_5.

The bulk susceptibility of the system rises as one proceeds from copper towards yttrium reaching its largest value at YCu_2. Interestingly enough, this coincides with a large rise in the yttrium Knight shift. The yttrium shift at YCu_2 is significantly larger than those in adjacent phases and larger than the value in pure yttrium. The small temperature dependence of the paramagnetism indicates that it is derived in the main from "non-d" electrons and although the crystal structure is not determined, one is led to conclude that a large rise in the density of states takes place at this phase stoichiometry.

Copper Resonances in Yttrium-Copper System

Copper (63) is a 70% abundant isotope with a nuclear spin 3/2. The 30% abundant isotope also has a nuclear spin of 3/2. Both nuclei have nearly identical magnetic moments and quadrupole moments. Copper (63) nuclear resonances were observed in four yttrium-copper phases and these are listed in Table 1. No quadrupole interactions were observed despite the fact that the symmetry of some of the phases permitted the existence of electric field gradients. Domagala (15) has ascertained the crystal structure of YCu_4 to be hexagonal. The copper nuclear resonance observed in this phase had a Knight shift which was independent of frequency and no satellites were observed. This indicates the absence of quadrupole effects which in this view would indicate the wrong assignment of crystal structure. Further, since YCu_6 is determined to be hexagonal it is quite probable that YCu_5, if it exists, is also hexagonal. As in the case of YCu_4 no quadrupole effects are observed.

The interpretation of the variation of the copper Knight shift is a bit difficult. There is no rise in the copper shift corresponding to the rise in the yttrium shift in the vicinity of YCu_2. Further, all the shifts are lower than the shift in pure copper metal despite a rise in the bulk susceptibility.

Yttrium Resonances in Yttrium-Nickel System

The formation of phases in the yttrium-nickel system has been studied by Domagala (15) and Beaudry (2). There are nine phases formed in the system extending in the nickel rich region up to Y_2Ni_{17}. Data on the yttrium Knight shift were obtained on six phases through Y_2Ni_7. No resonances were observed in YNi_4, YNi_5, and Y_2Ni_{17}. All the samples were very brittle and crushed with a mortar and pestle in a nitrogen atmosphere. The Knight shift data and the bulk susceptibilities are given in Table 1. The electron/atom ratio is calculated on the assumption that yttrium contributes three electrons to the conduction band and that nickel contributes eight.

The temperature dependence of the susceptibilities of YNi, YNi_2 and YNi_3 are given in Figures 2, 3, and 4, respectively. Only YNi indicates a behavior similar to a Curie-Weiss curve and for this the inverse susceptibility and the extrapolation to an ordering temperature are given. No other parameters indicated the presence of an ordering temperature. The susceptibility of YNi_2 was observed to have a field dependence typical of a sample with ferromagnetic impurities although the sample was cleaned with a magnet to remove ferromagnetic impurities. The presence of a ferromagnetic impurity as a second phase is unlikely since the neighboring phases in the system are not ferromagnetic. Only nickel itself is

ferromagnetic in the system. No other field dependent susceptibilities were observed in the yttrium-nickel system.

The main characteristics of the system, particularly the nickel rich portion, are the following. Despite changes in the crystal structure from phase to phase there is a steady increase in the yttrium Knight shift amounting to a 150% change over pure yttrium metal. There is a negligible temperature dependence to all the yttrium Knight shifts. There is a steady increase in the paramagnetic susceptibility as one approaches the nickel rich portion of the system. And finally, the susceptibilities are strongly temperature dependent in the nickel rich portion of the system.

Estimates of the band structure of nickel metal lead one to the conclusion that there are 0.6 electron holes in the d-band. This is discussed by Kittel (27). If one removes the interaction which produces the ferromagnetism in nickel and calculates the susceptibility arising from 0.6 electron holes and a spin-only assumption, one obtains at room temperature a gram susceptibility of 100×10^{-6}. This is of the order of magnitude of the susceptibility obtained for the nickel-rich yttrium-nickel phases. A final point is that the susceptibility of YNi_3 exceeds this estimate by a factor of four and the susceptibility of Y_2Ni_7 is slightly less than that of YNi_3. This estimate of the susceptibility of Y_2Ni_7 arises from a comparison of the behavior of the sample in a

large field gradient.

It appears reasonable to assume then that, neglecting the effects of changes in crystal structure, as one progresses towards nickel in the yttrium-nickel system both s and d electrons occupy levels of increasing density of states, as evidenced by the increasing susceptibility and the increasing yttrium Knight shift. The phase YNi_3 represents the phase of largest d-electron density of states with subsequent phases probably showing smaller susceptibility values as pure nickel is approached. The lack of resonance data for those phases very close to pure nickel limit our discussion of the s-electron density.

The chief difficulty with this explanation of the situation is that the yttrium Knight shift is practically temperature independent. Clogston (10) has shown that if the Fermi level intersects a conduction band made up of s and d character the properties dependent on the s-electron density of states will exhibit to some degree the temperature dependence of the d electrons. Clogston (10) cites several examples where the Knight shift is a linear function of the susceptibility, both changes brought about by a change in temperature.

Clearly, this contradicts the above explanation of the behavior of the yttrium-nickel system unless the s and d energy levels can be separated. In a discussion concerning itself

with the number of electrons in the 3 d band of iron, Weiss (51) arrives at the conclusion that there are two d electrons in iron and that these two magnetically active 3 d electrons occupy states which are below the Fermi surface of the conduction band. He further states that the reason these states are not fully occupied, although they are below the Fermi level, is the large correlation energy between electrons in the same localized state and that it is perhaps more favorable to leave the state empty if they are not too far below the Fermi level.

In view of the scanty evidence for such a situation in the yttrium-nickel system this view is somewhat tenuous. However, it is difficult to simultaneously satisfy the condition of a large temperature dependent paramagnetism and a large temperature independent Knight shift without some separation of the levels.

Yttrium Resonance in YMn_2

The yttrium-manganese system has been investigated by Myklebust (39). Three phases are formed, YMn_2, YMn_4, and YMn_{12}. YMn_4 is known to be ferromagnetic below 200 °C and no resonance was observed. No resonance was observed in YMn_{12}, no doubt due to the low concentration of yttrium. YMn_2 was sufficiently brittle to reduce to powder with a mortar and pestle in a nitrogen atmosphere. The sample was not annealed.

The experimental results for the yttrium Knight shift are given in Table 1 and the temperature dependence of the Knight shift is given in Figure 5. The susceptibility is listed in Table 1 and the temperature dependence is plotted in Figure 6. The field dependence of the susceptibility may arise from the presence of small quantities of the ferromagnetic YMn_4 phase, although the sample was prepared with a slightly yttrium rich stoichiometry which ordinarily would preclude such an occurrence.

Negative Knight shifts, such as those occurring here, have been explained using the concept of "core polarization". In the presence of polarized 3d electrons, there is an electrostatic attraction between these electrons and inner s core electrons of parallel spin. This results in a non-vanishing value of the quantity $|\psi_{MS\uparrow}(0)|^2 - |\psi_{MS\downarrow}(0)|^2$ which determines the effective field at the nucleus. $|\psi_{MS\uparrow}(0)|^2$ is the probability density of an s-wave function at the nucleus where M refers to the particular shell in question and $\uparrow$ or $\downarrow$ refer to the spin up or spin down sense of the electron in that shell. Core polarization has also been invoked to explain the "negative" fields in pure ferromagnetic metals by Hanna (21), Goodings (20), Jaccarino (24), Cohen (11), and Heine (23).

It is also possible for the interaction to make itself felt via the conduction electrons. If the d-electron

polarization can induce a negative polarization of the conduction electrons, then via the hyperfine interaction, which is the same mechanism for the Knight shift, it would be possible to obtain negative "effective" fields at the nucleus.

This latter case has been discussed by Clogston (10). The results for the temperature dependence of the yttrium Knight shift are not correlated with the temperature dependence of the susceptibility. This tends to weaken the argument for conduction electron polarization.

Scandium Resonances in Scandium Metal and Scandium-Yttrium Alloys

The nuclear magnetic resonance of scandium (45) was first observed by Blumberg (8) who reported the magnitude and temperature dependence of the Knight shift and further reported the absence of quadrupole effects and other magnetic effects such as anisotropic Knight shift. The scandium (45) nuclear resonance was observed in the scandium-yttrium alloys and at all concentrations the following interactions were observed: isotropic Knight shift, anisotropic Knight shift, and quadrupole effects. Because of the complexity of the analysis of the resonance line shape and position into the component factors, it will suffice to discuss in detail the treatment of the data for pure scandium metal. The parameters

for the alloys were obtained by an identical treatment except where otherwise specified.

The observation of quadrupole satellites provides an unambiguous evaluation of the quadrupole coupling provided the coupling is not too large. Upon application of high radio frequency power and large modulation field to a sample of pure scandium metal, two pairs of satellites as well as a distorted central resonance were observed. No satellites were observed in the alloys. The nuclear spin of scandium (45) is 7/2 and for this spin value one should observe three pairs of satellites. At no frequency of operation were more than two pairs of satellites observed. The correct assignment of satellite transitions was made using the following argument. The ratio of successive frequency spacings of corresponding satellites should be as 1:2:3. That is,

$$1\Delta\nu\,[(5/2 \longleftrightarrow 3/2) - (-3/2 \longleftrightarrow -5/2)] = 2\Delta\nu\,[(3/2 \longleftrightarrow 1/2) - (-1/2 \longleftrightarrow -3/2)]\ , \tag{31}$$

$$2\Delta\nu\,[(7/2 \longleftrightarrow 5/2) - (-5/2 \longleftrightarrow -7/2)] = 3\Delta\nu\,[(5/2 \longleftrightarrow 3/2) - (-3/2 \longleftrightarrow -5/2)]\ . \tag{32}$$

Because the spacing of the observed satellites was 1:2 one

concludes that it is the pair of 7/2 $\longleftrightarrow$ 5/2 satellites that is missing. If one were to argue that the 3/2 $\longleftrightarrow$ 1/2 satellites were obscured by the central transition, the observed satellite spacings should be as 2:3. This is not observed.

From satellite spacings at various frequencies, the quadrupolar coupling constant was determined to be 2.20 Mcps at room temperature. The various parameters for pure scandium and the scandium-yttrium alloys are listed in Table 4.

In order to obtain values of the Knight shift and anisotropic Knight shift it is necessary to study in detail the variation of the apparent line width of the central resonance as a function of frequency. For pure scandium the frequency range with a useful signal to noise ratio was 3 - 16 Mcps. Somewhat smaller frequency ranges were used with the alloys. At all times, the modulation amplitude was less than one-fourth the apparent line width to prevent modulation broadening. Further, estimates of the radio frequency saturation level were made and the power applied to the sample was held below those levels.

A plot of $\nu_o \Delta\nu$ vs ν_o^2 was made and is shown in Figure 7. The equation which represents this straight line is one of the following:

$$\nu_o \Delta\nu_{HL} = \frac{25\,b}{9} - \frac{5\,a}{3\,\nu_o^2} \quad , \tag{33}$$

$$\nu_o \Delta\nu_{HS} = \pm\,(b - 3a\,\nu_o^2) \quad . \tag{34}$$

These equations are simply algebraic rearrangements of Equations 25, 26, and 27. The substitution of ν_o for ν_{iso} has been made. Using Equation 33 we obtain a value of 2.05 Mcps for the coupling constant, in good agreement with satellite splitting. This corresponds to a value of the parameter b equal to 20.1×10^{-3} Mcps^2. Also from Equation 33, we obtain a value of a equal to -0.041%. The line drawn in Figure 7 is a least squares fit to the data point and the parameters are determined analytically. For the values of a and b obtained, it is found that Equation 33 satisfies the validity criterion given in Equation 26. This method of using a $\nu\Delta\nu$ vs ν^2 plot will be referred to as method A.

From Equations 28 and 29, it can be seen that we can arrive at some value of the isotropic Knight shift. K_H and K_L are plotted vs $1/\nu^2$ in Figure 8. From the slope of K_H we obtain a value of b equal to 16.3×10^{-3} Mcps^2. The infinite frequency intercepts of both K_H and K_L provide the following equations:

$$K_H(\nu = \infty) = K_{iso} - a \quad , \tag{35}$$

$$K_L(\nu = \infty) = K_{iso} + \frac{2a}{3} \quad . \tag{36}$$

Using a value of a obtained in method A and applying it to K_H, one obtains a value of K_{iso} equal to 0.222% at 300 °K. This method of obtaining both an estimate of b and a value of K_{iso} using the value of a obtained in method A will be known as method B. Finally, using the pair of Equations 35 and 36, one can obtain independently the values of a and K_{iso}. For the 300 °K pure scandium data as shown in Figure 8 this leads to a equal to -0.039% and K_{iso} equal to 0.224%.

This method of analysis was used for all the solid solution alloys of scandium and yttrium and the data is summarized in Table 4. For purposes of clarification, the $\nu\Delta\nu$ vs ν^2 plot of the alloys is illustrated in Figure 9. It should be noted that all the plots use the notation ν instead of ν_o since they are analytically inseparable. The best values of the scandium (45) isotropic Knight shifts are plotted as a function of composition in Figure 1. The values of the anisotropic Knight shifts (these values are practically identical to the value of the parameter a) as determined from method A are plotted as a function of composition in Figure 10. The values of the quadrupole coupling constants as derived from method A are plotted as a function of composition in Figure 10.

Beaudry (3) has also determined the lattice parameters of the scandium-yttrium system. By separately smoothing the data for the lattice parameters a and c (the conventional

symbols for hexagonal crystal lattice parameters are being used), and obtaining the values of a and c/a for a representative number of concentrations across the scandium-yttrium system, it is possible to obtain the lattice contribution to the quadrupolar coupling constant for the scandium (45) nucleus. A non-cubic lattice of point ions has a non-vanishing electric field gradient at the lattice sites. It is this gradient alone which is what one calls the lattice field gradient, or sometimes the ion-background gradient. Das (13) and DeWette (14) give the following equation for determining the lattice field gradient:

$$\begin{aligned} q(\text{lattice}) &= q_L \\ &= [0.0065 - 4.3584(c/a - 1.633)] \,/\, a^3 \quad . \end{aligned} \tag{37}$$

To further calculate the coupling constant one must also know the degree of ionization of each atom, Z, and the Sternheimer "antishielding" factor, γ_∞ . The lattice coupling constant is then given by

$$\frac{e^2 q_L Q(Sc^{45}) \left[1 + \gamma_\infty\right] Z}{h} \tag{38}$$

where h is Planck's constant and e is the electron charge. The values assumed by Das (13) of Z equal to three and γ_∞ equal to seven are also taken here. For the quadrupole

moment $Q(Sc^{45})$ a recent determination by Fricke (17) from optical hyperfine structure yields a value of 0.22 barns. One then obtains a value of the lattice contribution to the coupling constant for pure scandium metal of 1.06 Mcps. The variation of the lattice contribution to the coupling constant of scandium (45) across the scandium-yttrium system is indicated in Figure 10. Since the above assumptions are being applied to the scandium-yttrium system, it is implicit that the degree of ionization of the yttrium atoms is identical to that of the scandium atoms.

There have been many experiments performed with nuclear magnetic resonance in which the nuclear resonance of a given atom is observed while a different atom is introduced into the lattice. Naturally these experiments are only valid in the concentration regions where the two atoms form a solid solution. In the classic experiment of Bloembergen (7), the nuclear resonance of copper was observed while the neighboring atom in the periodic table, zinc, was introduced into the lattice. Copper has a nuclear spin of 3/2 and a large quadrupole moment. The copper crystal structure is face-centered cubic thereby precluding field gradients at the nuclear sites and hence no quadrupole interaction with the copper nuclei is observed. As zinc atoms are introduced into the lattice, the copper nuclear resonance broadens only slightly but diminishes in intensity and disappears completely at 12 - 15%

zinc content. This experiment and others (Blandin (5)) have been interpreted as a combination of two effects. As atoms of different size are introduced into the cubic lattice, strains develop which destroy the cubic symmetry locally. The resulting field gradients are then presumed sufficiently large to extract from the copper central resonance intensity that portion of the intensity which comes from the no longer degenerate satellite transitions ($\pm$ 3/2 $\longleftrightarrow$ $\pm$ 1/2). The field gradients are presumed also to be sufficiently non-uniform so that the satellites themselves are rendered unobservable; that is, there is a spectrum of field gradient values which in turn produce a spectrum of satellite transition frequencies.

The second contribution to the disappearance of the resonance is the valence or charge effect. It was felt that sufficiently large field gradients could not be obtained solely from lattice distortion and that another source of field gradients might be from the excess charge on the impurity atom. Rowland (45), Friedel (19), Blandin (5), Langer (34), Kohn (33) and Sagalyn (47) have been able to calculate these valence effects with the conclusion being that there are long range oscillations of the charge density of the screening conduction electrons around the impurity atom. Rowland (45) concluded that the origin of electric field gradients around multivalent solutes in copper

is almost purely an effect of conduction electron distribution and that inhomogeneous strains introduced by solutes had a relatively slight effect on the gradients in most of the alloys investigated. Sagalyn (47) concluded that the relative effects of valence and strain differ depending on the solute atom in question.

On the other hand, there is considerable evidence for essentially zero contribution from both valence and strain effects. Barnes (1) has observed the vanadium (51) nuclear resonance in body-centered cubic alloys of vanadium and chromium across the entire system. Vanadium (51) has a large quadrupole moment but there are no observable quadrupole effects in either line width or intensity. Van Ostenburg (49) has observed the vanadium (51) resonance in the body-centered cubic solid solutions of V-Ti, V-Cr, and V-Tc. The last system he has also observed the technetium (99) resonance and technetium (99) also has a large quadrupole moment.

Two characteristics of these "non-effect" cases are that only transition elements are involved and the atomic radii of the atoms involved is small. There is a 6% difference in atomic radius between vanadium and chromium, 1% between vanadium and technetium, and 9% between vanadium and titanium.

If one accepts the data shown in Figure 4, one is then accepting the reality of a definite value of gradient

which is nearly the same for each and every scandium (45) nuclear site, although that alloy is presumed to be a random solution. That the field gradients are not all the same is evidenced by the failure to observe the satellites which are sensitive to non-uniformity in the field gradient value. The central resonance is not nearly so sensitive. In his work on the scandium-yttrium system, Beaudry (3) states that the samples were given homogenizing anneals at 550 ^{o}C for fifteen hours and that the X-ray data were interpreted unequivocally. For a hexagonal system evidence for ordering from an X-ray analysis comes only in the variation of intensities of the lines in the diffraction pattern rather than from the appearance of super-lattice lines. No unusual intensity variations were noted nor were any anomalies noted in the thermal analysis. The conclusion is that at present there is no evidence for ordering in the scandium-yttrium system and that we arrive at some definite and uniform value of the field gradient for each alloy because of the similarity in size of the two atoms (there is a 11% difference in the metal radii of scandium and yttrium which is approximately the difference in their atomic radii) and because of some charge shielding mechanism which is poorly understood.

An important fact to be noted is that the lattice contribution to the field gradient is approximately constant across the system. The variation in the lattice parameters

a and c/a is such that the net change in field gradient as calculated by Equation 37 is extremely small in going from pure scandium to pure yttrium. Yet the experimentally observed field gradient changes by more than a factor of two.

In the case of beryllium metal it has been shown by Pomerantz (41) that the contribution to the total field gradient from the electronic distribution is approximately 8%. This implies that the conduction electrons are not completely free electrons since completely free electrons cannot produce an orientation dependent interaction. The electronic contribution to the electric field gradient is a measure of the non-spherical electronic distribution in real space.

Via the anisotropic Knight shift parameter, it is possible to measure the quadrupole moment of the electrons near the Fermi surface (Bloembergen (7)). It is possible then in the scandium-yttrium system to correlate changes in the electronic distribution in real space with changes in electronic distribution in reciprocal or momentum space.

If one defines the parameter Δ as

$$\Delta = \begin{pmatrix}\text{experimentally observed}\\ \text{coupling constant}\end{pmatrix} - \begin{pmatrix}\text{lattice contribution}\\ \text{to coupling constant}\end{pmatrix}, \quad (39)$$

then this parameter measures the contribution to the field gradient from sources other than the lattice. In Figure 11 the Knight shift anisotropy of a given alloy is plotted vs.

$\Delta^{1/2}$ for that alloy. Each point represents a different alloy. The choice of 1/2 for the power of Δ was empirical. It appears then that for the scandium-yttrium system there is a linear relationship between the anisotropic Knight shift and the square root of Δ.

Drain (16), in connection with nuclear magnetic resonance in silver-cadmium alloys, has given an expression which connects the density of states in the alloy to the Knight shift in the alloy. This expression is

$$N(E_F) = (1-c)N_A(E_F)\ K_A/K_{AA} + cN_B(E_F)\ K_B/K_{BB} \quad , \qquad (40)$$

where K_{AA} and K_{BB} are the Knight shifts in the pure metals, $N(E_F)$ refers to the density of states in the alloy, $N_A(E_F)$ and $N_B(E_F)$ refer to the density of states in pure metals A and B respectively, K_A and K_B refer to the Knight shift of A and B respectively in the alloy and c is the mole fraction. The density of states is related to the electronic specific heat by Equation 6. The electronic specific heat of scandium and yttrium has been measured by Montgomery (38). The results for scandium are γ = 11.3 millijoules/mole-$^oK^2$ and for yttrium γ = 10.2 millijoules/mole-$^oK^2$. These values are plotted in Figure 1. The line is the straight line connecting the values for scandium and yttrium. The intermediate points are calculated from Equation 40.

Manganese Resonances in YMn_2

In a sample of YMn_2 at 300 °K six resonances other than the previously discussed yttrium resonance were observed. All six resonances were attributed to the manganese (55) nucleus. Three resonances were identified as satellites, two were identified as the split central transition, and one was thought to represent the step resonance. One satellite, the $m = +3/2 \longleftrightarrow m = +5/2$ transition, was not observed. At 15.500 Mcps the resonance pattern extended 3500 gauss with the central resonance split by 600 gauss. Because of the extent of the resonance pattern no figures are given but the raw data is given in Table 5. Further, because of the large splitting of the central resonance it is no longer valid to equate ΔH with $\Delta \nu$. To avoid errors involved in the transformation from field splittings to frequency splittings, the data was plotted on a frequency vs. magnetic field plot and the frequency splittings were read off for various constant field cuts.

At 77 °K much the same resonance pattern was obtained. All four satellites were observed although no measurements were made on the $m = -5/2 \longleftrightarrow m = -3/2$ transition. The central resonance was observed to be split by 600 gauss at 15.500 Mcps. No resonance corresponding to the step was observed. The 77 °K data is given in Table 6.

The data present a significant deviation from the expected behavior. There is a slight curvature of satellite lines which at low fields can be attributed to higher order perturbation terms. However the asymptotes of these satellite lines at high fields have different slopes whereas Equation 30 predicts that they should have the same slope. Extrapolation of the ($-3/2 \longleftrightarrow -1/2$) and ($1/2 \longleftrightarrow 3/2$) slopes to zero field should yield intercepts of $+\nu_Q$ and $-\nu_Q$ respectively. That is, the average value of the intercepts should be zero. This does not occur. Further, the resonance attributed to the step should pass through the origin according to Equation 24. This does not occur. And finally, when K_L and K_H are plotted vs. $1/\nu^2$, K_H has a significant curvature at high frequencies whereas K_L is straight. Because of an explicit dependence on higher order terms as given by Equation 29, one might have expected K_L to be curved. The equation for K_H contains no such dependence.

If one allows for the existence of small internal magnetic fields whose magnitude and sign are orientation dependent, it is possible to arrive at a set of parameters which are more consistent than parameters derived from the raw data. For the 300 ^{o}K data the average intercept at zero external magnetic field for the ($-3/2 \longleftrightarrow -1/2$) and ($+1/2 \longleftrightarrow +3/2$) satellite transition asymptotes is 0.243 Mcps. Using a value of slope equal to the average of the

slopes of the asymptotes and extrapolating to zero frequency one obtains a value of magnetic field equal to -235 gauss. It should be remembered that the satellite transitions correspond to 90° intensity maxima. This implies then that to read "correct" frequency values for resonances corresponding to 90° maxima one should read them from the frequency vs. magnetic field plot at a value of H-235 gauss, where H represents the magnetic field value desired. All resonances except ν_L and ν_S are 90° resonances.

If one forces a least squares derived straight line through the step resonance data one obtains a zero frequency intercept of +364 gauss. This implies then that to read "correct" frequency values for resonances corresponding to zero degree maxima (this is the angular orientation of the step intensity maximum) one should read them from the frequency vs. magnetic field plot at a value of H+364, where H represents the magnetic field desired. Unfortunately, in a powder sample the only resonance corresponding to zero degrees is the step resonance.

The pattern that emerges from this analysis is that if one allows the existence of an internal field, such a field in YMn_2 provides a negative contribution of 364 gauss at zero degree orientations and a positive contribution of 235 gauss at 90° orientations. If we further assume that the internal field contribution is zero near the middle of the

angular range of concern, more specifically 45°, then it can be seen that there will be essentially zero contribution to the ν_L resonance, which corresponds to an intensity maximum of 42°.

There are several defects to the above assumptions which will be discussed presently. The advantages are a set of parameters which are reasonably internally consistent and which do not seem unreasonable when compared to analogous examples. From satellite splitting at large magnetic field, thereby minimizing higher order perturbation corrections, a value of ν_Q equal to 2.41 Mcps is obtained which corresponds to a coupling constant of 16.1 Mcps. Using a set of "corrected" ν_H values, a plot of $\nu\Delta\nu_{HL}$ vs. ν^2 yields a zero frequency intercept corresponding to a ν_Q of 2.32 Mcps. The slope of the straight line of such a plot yields a value of a or K_{ax} equal to +0.65%. Further, a plot of K_L and K_H vs. $1/\nu^2$ now yields straight lines for both. Using the pair of Equations 35 and 36, one obtains a value of K_{ax} equal to +0.69% and K_{iso} equal to -1.14%. The slope K_L yields a value of ν_Q equal to 2.35 Mcps. However, the slope of K_H yields a value of ν_Q equal to 4.17 Mcps. An analysis of the 77 °K data was not made but estimates indicate that K_{ax} is less positive and K_{iso} is less negative. Satellite splitting of the 77 °K data indicate a quadrupole coupling of 16.9 Mcps.

The origins of the effective internal fields that are

assumed are not understood. The susceptibility data of YMn_2, as given in Figure 6, indicate a field dependence but obvious ferromagnetic or anti-ferromagnetic ordering. The susceptibility data has been taken up to 200 °C, not indicated in Figure 6, with no indications of ordering. If there is indeed some undetected ordering of the electrons, it is difficult to understand why the value of the internal fields are so small and why it has the angular dependence that it appears to have.

The cubic laves phase structure of YMn_2 has been given by Beaudry (3) where a_o, the cell dimension, is assigned the value of 7.68 A^o. Jones (25) has given the formula for calculating the field gradients at the B sites of the cubic laves phase AB_2 type compounds as

$$q(\text{lattice}) = q_L = \frac{1}{a_o^3}\left[-53.8\ n_A + 115.7\ n_B\right] , \tag{41}$$

where n_A and n_B are the charge of the A and B atoms respectively. Using plus three as the charge on the yttrium atom and plus two as the charge on the manganese atom one obtains $q_L = 1.55 \times 10^{23}$ cm^{-3}. Omitting the antishielding factor for the moment one obtains a theoretical lattice coupling constant $e^2 q_L Q(Mn^{55})/h = 2.96$ Mcps. Leighton (35) gives the quadrupole moment of manganese (55) as 0.55 barns. Burns (9) has given the antishielding factor of manganese

doubly-positive ion as $\gamma_\infty(Mn^{++}) = 6.8$. Using $(1 + \gamma_\infty) = 7.8$ to estimate the lattice coupling constant we arrive at a value of $e^2Q(Mn^{55})q_L(1+\gamma_\infty)/h = 23.1$ Mcps, to be compared with an experimental coupling constant of 16.1 Mcps.

Previous examples of quadrupole interactions in cubic laves phases given by Jones (26) indicate that the lattice coupling constant exceeds the experimental value by roughly 50%. Apparently in these cases, the non-lattice contribution cancels some of the lattice contribution resulting in smaller experimental values. One could bring the theoretical lattice coupling for the manganese more in agreement with the work by Jones (26) by increasing slightly either the manganese quadrupole moment or the antishielding factor. Conversely, one could bring the theoretical lattice coupling into agreement with the experimental coupling by reducing either the manganese quadrupole moment or the antishielding factor.

SUMMARY

Using nuclear magnetic resonance techniques on systems of yttrium and transition elements combined with paramagnetic susceptibility data, a variety of useful parameters including isotropic Knight shifts, anisotropic Knight shifts, nuclear electric quadrupole coupling constants, and estimates of band structure have been obtained.

In the systems yttrium-copper and yttrium-nickel, interpretation of the variation of the yttrium Knight shifts is impeded by the presence of phases of different crystal structures. However, correlations with the paramagnetic susceptibility have been made which, when combined with the temperature dependences of both the susceptibility and the Knight shift, shed some light on the properties of the band structures of these phases.

Very little information has been derived from the copper Knight shifts in the yttrium-copper system. However, the fact that no quadrupole interactions are observed in connection with the copper resonance in YCu_4 would indicate that the hexagonal crystal structure assignment to that phase is in error.

The Knight shift of yttrium in YMn_2 was observed to be very large and negative. The temperature dependence of this Knight shift was measured at intervals between 77 ^{o}K and

300 ^{o}K and evidenced a positive slope. An explanation of this negative Knight shift was given in terms of core polarization.

The Knight shift of yttrium in yttrium metal and yttrium-scandium alloys was measured. The yttrium Knight shift was seen to follow a linear variation of the density of states connecting pure yttrium and pure scandium. The temperature dependence of the shifts were measured and corrected previous conclusions by other authors.

The Knight shift, anisotropic Knight shift, and quadrupole coupling of scandium (45) in pure scandium metal and scandium-yttrium alloys were measured. The results obtained for the Knight shift and its temperature dependence in pure scandium metal were similar to results obtained previously by other authors. The values of the quadrupole coupling and anisotropic shift parameters were not obtained by these authors and are reported here for the first time. In addition, from the values of the lattice parameters for pure scandium metal, estimates of the lattice contribution to the quadrupole coupling are given.

In the scandium-yttrium alloys, definite values of electric field gradient are observed for the scandium nuclear sites. Further, the non-lattice contributions to the field gradients at the scandium (45) nuclear sites are correlated with the anisotropic Knight shift for the same nuclei.

The manganese (55) nuclear resonance was observed in YMn_2. The Knight shift and the anisotropic Knight shift were estimated. In addition, the first manganese (55) nuclear electric quadrupole interaction was observed. Evidence is given for the existence of weak internal magnetic fields which are orientation dependent. The currently accepted values for the manganese (55) quadrupole moment and antishielding factor seem appropriate.

LITERATURE CITED

1. Barnes, R. G. and Graham, T. P. Nuclear magnetic resonance in chromium metal. Physical Review Letters 8:248. 1962.

2. Beaudry, B. and Daane, A. Yttrium-nickel system. Transactions of the American Institute of Metallurgical Engineers 218:854. 1960.

3. Beaudry, B. and Daane, A. [Yttrium-copper and yttrium-scandium systems.] [Unpublished manuscript.] Ames, Iowa, Dept. of Chemistry, Iowa State University of Science and Technology. 1962.

4. Beaudry, B.; Haefling, J.; and Daane, A. Some laves phases of yttrium with transition metal elements. Acta Crystallographica 13:743. 1960.

5. Blandin, A.; Daniel, E.; and Friedel, J. Sur le deplacement de Knight dans les alliages. Journal of Physics and Chemistry of Solids 10:126. 1959.

6. Bloch, F. Nuclear induction. Physical Review 70:460. 1946.

7. Bloembergen, N. and Rowland, T. J. On the nuclear magnetic resonance in metals and alloys. Acta Metallurgica 1:731. 1953.

8. Blumberg, W.; Eisinger, J.; Jaccarino, V.; and Matthias, B. Nuclear magnetic resonance in scandium and lanthanum metal. Physical Review Letters 5:52. 1960.

9. Burns, G. and Wikner, E. Antishielding and contracted wave functions. Physical Review 121:155. 1961.

10. Clogston, A. and Jaccarino, V. Susceptibilities and negative Knight shifts of intermetallic compounds. Physical Review 121:1357. 1961.

11. Cohen, M.; Goodings, D.; and Heine, V. Contribution of core polarization to the atomic hyperfine structure and Knight shift of Li and Na. Proceedings of the Physical Society (London) 73:811. 1959.

12. Cohen, M. and Reif, F. Nuclear quadrupole effects in solids. Solid State Physics 2:239. 1956.

13. Das, T. P. and Pomerantz, M. Nuclear quadrupole interactions in pure metals. Physical Review 123:2070. 1961.

14. DeWette, F. Electric field gradients in point-ion and uniform background lattices. Physical Review 123:103. 1961.

15. Domagala, R.; Rausch, J.; and Levinson, D. The systems Y-Fe, Y-Ni, and Y-Cu. American Society of Metals Preprint 187. 1960.

16. Drain, L. Nuclear resonance in silver-cadmium. Philosophical Magazine 4:484. 1959.

17. Fricke, G.; Kopfermann, H.; Penselin, S.; and Schlupmann, K. Bestimmung der Hyperfeinstrukturaufspaltung der Scandium-Grundzustande $^2D_{3/2}$ und $^2D_{5/2}$ und des Quadrupolmomentes des Sc^{45}-Kernes. Naturwissenschaften 46:106. 1959.

18. Friedel, J. Distribution of electrons round impurities in monovalent metals. Philosophical Magazine 43:153. 1952.

19. Friedel, J. Metallic alloys. Supplement Nuovo Cimento 7:287. 1958.

20. Goodings, D. and Heine, V. Contribution of exchange polarization of core electrons to the magnetic field. Physical Review Letters 5:370. 1960.

21. Hanna, S.; Heberle, J.; Perlow, G.; Preston, E.; and Vincent, D. Direction of the effective magnetic field at the nucleus in ferromagnetic iron. Physical Review Letters 4:513. 1960.

22. Hansen, W. H. Some low temperature magnetic and thermal properties of the chromium (III) halides. Unpublished Ph.D. thesis. Ames, Iowa, Library, Iowa State University of Science and Technology. 1956.

23. Heine, V. Hyperfine structure of paramagnetic ions. Physical Review 107:1002. 1957.

24. Jaccarino, V.; Peter, M.; and Wernick, H. Nuclear magnetic resonance in α and β manganese. Physical Review Letters 5:53. 1960.

25. Jones, W. H., Jr.; Graham, T. P.; and Barnes, R. G. Knight shifts of potassium, yttrium, and indium. Acta Metallurgica 8:663. 1960.

26. Jones, W. H., Jr.; Graham, T. P.; and Barnes, R. G. Nuclear magnetic resonance line shapes resulting from the combined effects of nuclear quadrupole and anisotropic shift interactions. [Unpublished manuscript.] Ames, Iowa, Dept. of Physics, Iowa State University of Science and Technology. 1962.

27. Kittel, C. Introduction to Solid State Physics. 2nd ed. New York, N. Y., McGraw-Hill Book Co., Inc. 1960.

28. Knight, W. D. Nuclear magnetic resonance in metals. Solid State Physics 2:93. 1956.

29. Knight, W. D. Nuclear magnetic resonance shift in metals. Physical Review 76:1259. 1949.

30. Knight, W. D. Temperature dependence of nuclear resonance in metals. Physical Review 96:861. 1954.

31. Kohn, W. Interaction of conduction electrons and nuclear magnetic moments in metallic Li. Physical Review 96:590. 1954.

32. Kohn, W. and Kjeldaas, T. Interpretation of the Knight shift in metallic sodium. Physical Review 99:622. 1955.

33. Kohn, W. and Vosko, S. H. Theory of nuclear resonance intensity in dilute alloys. Physical Review 119:912. 1960.

34. Langer, J. S. and Vosko, S. H. The shielding of a fixed charge in a high-density electron gas. Journal of Physics and Chemistry of Solids 12:196. 1959.

35. Leighton, R. Principles of Modern Physics. New York, N. Y., McGraw-Hill Book Co., Inc. 1959.

36. McGarvey, B. R. and Gutowsky, H. S. Nuclear magnetic resonance in metals. Journal of Chemical Physics 21: 2114. 1953.

37. Meyerhoff, R. W. and Smith, J. F. Anisotropic thermal expansion of single crystals of thallium, yttrium, beryllium and zinc at low temperatures. Journal of Applied Physics 33:219. 1962.

38. Montgomery, H. and Pells, G. Low temperature specific heat of scandium and yttrium. Proceedings of the Physical Society (London) 78:622. 1961.

39. Myklebust, R. and Daane, A. The yttrium-manganese system. Transactions of the American Institute of Metallurgical Engineers 224:354. 1962.

40. Pake, G. E. Nuclear resonance absorption in hydrated crystals. Journal of Chemical Physics 16:327. 1948.

41. Pomerantz, M. and Das, T. P. Theory of nuclear quadrupole interaction in beryllium metal. Physical Review 119:70. 1960.

42. Pound, R. V. Nuclear electric quadrupole interactions in crystal. Physical Review 79:685. 1950.

43. Redfield, A. Nuclear magnetic resonance saturation in solids. Physical Review 98:1787. 1955.

44. Rowland, T. J. Nuclear electric quadrupole interactions in aluminum. Acta Metallurgica 3:74. 1955.

45. Rowland, T. J. Nuclear magnetic resonance in copper alloys. Physical Review 119:900. 1960.

46. Rowland, T. J. Nuclear magnetic resonance in metals. Progress in Materials Science 9:1. 1961.

47. Sagalyn, P.; Paskin, A.; and Harrison, R. Contribution of strain to nuclear quadrupole interactions in dilute alloys of copper. Physical Review 124:428. 1961.

48. Townes, C. H.; Herring, C.; and Knight, W. D. Effect of electronic paramagnetism on nuclear magnetic resonance frequencies in metals. Physical Review 77: 852. 1950.

49. Van Ostenburg, D.; Lam, D.; Trapp, H.; and Macleod, D. Knight shifts and susceptibilities in V alloys with Ti, Cr, and Tc. [Unpublished manuscript.] Argonne, Illinois, Argonne National Laboratory.

50. Webb, M. Knight shift and quadrupole effects in Al alloys. Journal of Physics and Chemistry of Solids 20:127. 1961.

51. Weiss, R. J. and Marshall, W. Electronic structure of transition metals. Journal of Applied Physics Supplement 30:220S. 1959.

ACKNOWLEDGEMENTS

The author wishes to express his appreciation to Dr. R. G. Barnes for his long friendship and assistance during the author's academic career.

Thanks are given to Dr. David Petersen for his encouragement and helpful suggestions.

Thanks are also extended to Mr. B. Beaudry who generously supplied many of the samples used in this research and Dr. T. Graham and Mr. A. Miller for interesting and valuable discussions.

APPENDIX

Table 1. Tabulation of yttrium Knight shifts (K_Y), copper Knight shifts (K_{Cu}) and gram susceptibilities for various phases studied

Phase	K_Y(%)[a]		K_{Cu}(%)[b]	Elec/	g(emu/g)x10^{-6}		Crystal
	300 °K	77 °K	300 °K	atom	300 °K	77 °K	structure
Cu			0.230[c]	1.0	0		f.c.c.
YCu_6	0.305 ± .005		- [d]	1.2	0.17	0.16	hex.[e]
YCu_5	0.274 ± .014		0.139 ± .002	1.3			?
YCu_4	-[f]		0.166 ± .005	1.4	2.3	2.4	hex.[e]
YCu_3	0.374 ± .005		0.163 ± .005				?
YCu_2	0.383 ± .005		- [d]	1.7	6.9	7.4	?
YCu	0.264 ± .005	0.253 ± .005	0.195 ± .003	2.0	0.78	0.76	Simple cubic (CsCl)[e]

[a] Reference compound $Y(NO_3)_3$.

[b] Reference compound CuCl.

[c] See Knight (29).

[d] Copper resonance not observed.

[e] See Domagala (15).

[f] Yttrium resonance not observed.

Table 1. (Continued)

Phase	K_Y(%)[a] 300 °K	K_Y(%)[a] 77 °K	K_{Cu}(%)[b] 300 °K	Elec/ atom	g(emu/g)x10^{-6} 300 °K	g(emu/g)x10^{-6} 77 °K	Crystal structure
Y	0.321 ± .003	0.300 ± .003		3.0	2.1	2.4	hex.[g]
Y_3Ni	0.335 ± .010	0.314 ± .014		4.3	1.6	1.5	?
Y_3Ni_2	0.384 ± .004	0.360 ± .010		5.0	2.2	1.2	?
YNi	0.214 ± .002	0.227 ± .005		5.5	13.2	27.8	Orthorhombic[e]
YNi_2	0.498 ± .003	0.497 ± .010		6.2	6.1	16.3	Cubic laves[e]
YNi_3	0.718 ± .010	0.680 ± .010		6.8	471.0	868.0	hex.[e]
Y_2Ni_7	0.739 ± .010	--[f]		7.0			?
YMn_2	-0.680 ± .004	-0.711 ± .015			136.0	172.0	Cubic laves[h]

[g]See Beaudry (3).

[h]See Myklebust (39).

Table 2. Impurities in the yttrium and scandium metal used to prepare the scandium-yttrium alloys, in parts per million

Element	Fe	Ta	C	Al	Ti	N	Mg	Si	Cu	Ni	Ca	Cr	O
Y	159	100	115	--	--	56	30	--	--	85	30	--	100
Sc	475	240	290	100	20	100	25	50	100	75	55	75	250

Table 3. Knight shift of yttrium (89) in yttrium-scandium alloys

Alloy	K_Y(%) at 300 °K	K_Y(%) at 77 °K
Pure Y	0.321 ± .003	0.300 ± .003
90.5% Y	0.327 ± .006	0.299 ± .006
80.1% Y	0.336 ± .003	0.318 ± .006
66.9% Y	0.337 ± .007	0.324 ± .011
50.0% Y	0.353 ± .010	---

Table 4. Scandium (45) parameters in the scandium-yttrium system determined in various ways.
F or scandium (45), $b = \frac{15}{3136}$ [coupling constant] ^{2}

Alloy composition	b from satellites $x10^{-3}$ Mcps^2	b from method A $x10^{-3}$ Mcps^2	b from method B $x10^{-3}$ Mcps^2	a from method A %	a from method C %	Kiso from method B %	Kiso from method C %	Freq. range invest. Mcps.
Pure Sc at 300 °K	23.2	20.1	16.3	-0.041	-0.039	+0.222	+0.224	3-16
Pure Sc at 77 °K	21.5	18.0	15.8	-0.049	-0.047	+0.253	+0.249	3-16
33.5% Y at 300 °K		33.1	14.7	-0.029	-0.025	+0.189	+0.193	4-16
50.0% Y at 300 °K		58.7	19.0	-0.018	-0.033	+0.195	+0.180	7-16
66.9% Y at 300 °K		98.7	61.5	-0.004	-0.001	+0.213	+0.216	7-16
80.1% Y at 300 °K		124.5	134.0	0	+0.030	+0.173	+0.203	7-16
90.1% Y at 300 °K		129.0	108.0	+0.001	+0.004	+0.197	+0.200	10-16
90.1% Y at 77 °K		154.0	137	+0.008	+0.024	+0.180	+0.200	11-16

Table 5. Experimental data for manganese (55) resonances in YMn_2 at 300 °K. Numbers in table are magnetic field values in gauss for frequencies given.

Transition frequency in Mcps	+3/2<->+1/2	ν_L	ν_S	ν_H	-1/2<->-3/2	-3/2<->-5/2	ν_R
15.500		15,162	15,044	14,643	13,542	12,561	14,688
14.000		13,755	13,621	13,184	12,101	11,162	13,266
13.500	13,940						12,792
13.000		12,839	12,683				
12.000		11,905	12,683	11,238	10,194		11,371
11.000		10,987	10,812				
10.000	10,531	10,073	9,883	9,284	8,293		9,475
9.000		9,189		8,308			8,528
8.000	8,569	8,293					7,580
7.000	7,608	7,412					6,633
5.000		5,725		4,336			4,738

Table 6. Experimental data for manganese (55) resonances in YMn_2 at 77 °K. Numbers in table are magnetic field values in gauss for frequencies given.

Transition frequency in Mcps	+5/2 ⟷ +3/2	+3/2 ⟷ +1/2	ν_L	ν_H	-1/2 ⟷ -3/2
15.500		15,890	15,174	14,597	13,437
14.000		14,438	13,778	13,140	12,011
12.000		12,497	11,932	11,190	10,073
8.055	9,503	8,629	8,390		6,301

Figure 1. Knight shifts for Y^{89} and Sc^{45} and density of states as a function of concentration in the yttrium-scandium system. The density of states in the system is plotted in the lower part of the graph. The density of states is measured in millijoules/mole-$^oK^2$. The straight line connects the values for pure scandium and pure yttrium. The other points are calculated from Equation 40.

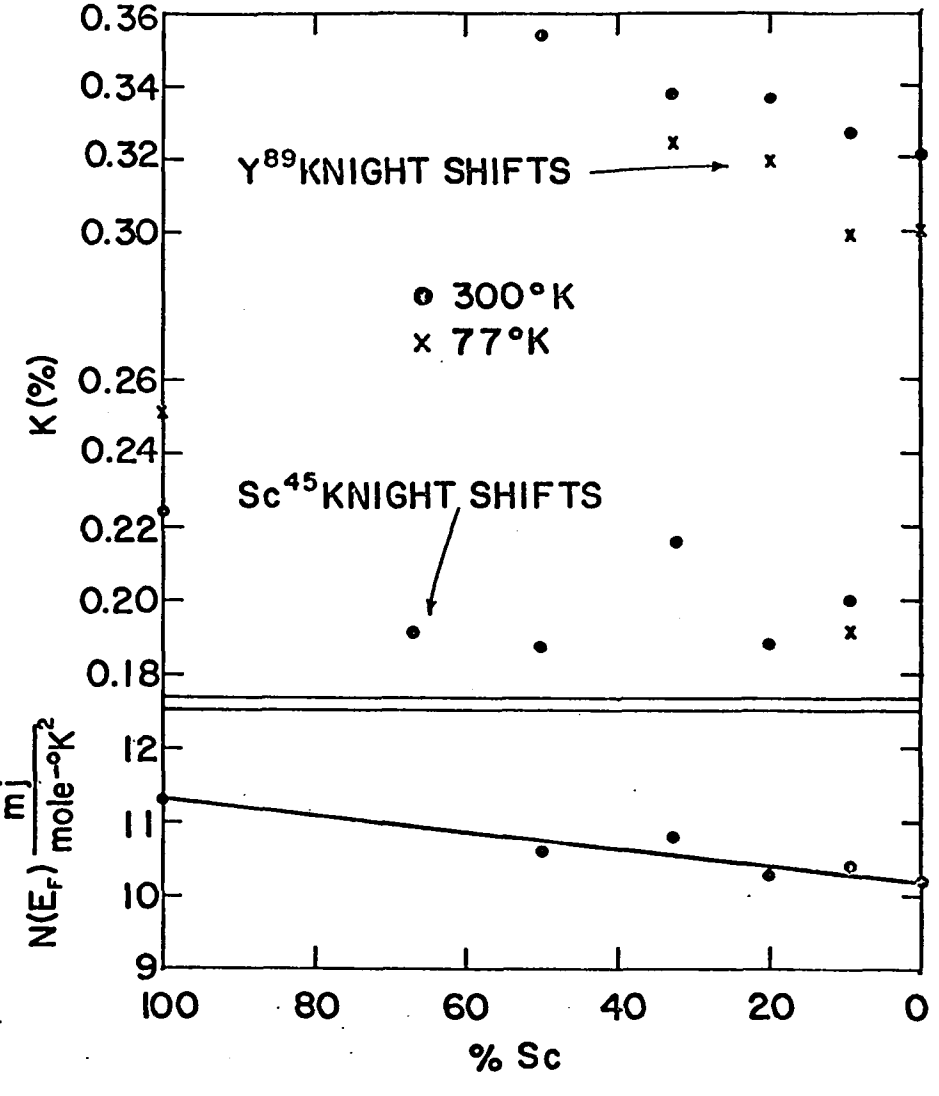
0.36
0.34
0.32
0.30
0.26
0.24
0.22
0.20
0.18
K (%)
Y89 KNIGHT SHIFTS
300°K
77°K
Sc45 KNIGHT SHIFTS
12
11
10
9
N(EF) mj/mole-°K2
100
80
60
40
20
0
% Sc

Figure 2. Temperature dependence of the gram susceptibility and inverse gram susceptibility of YNi

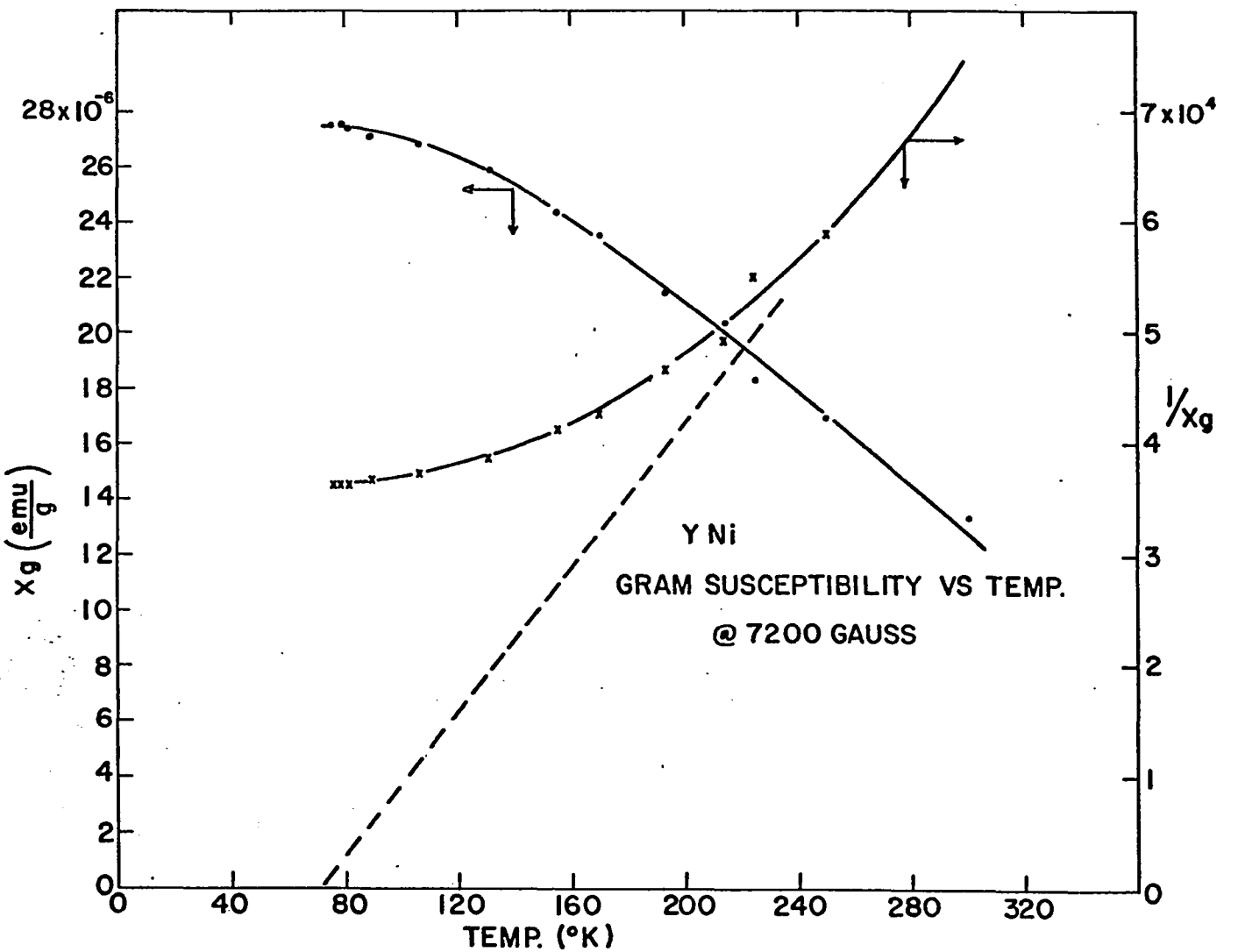
28x10⁻⁶
26
24
22
20
18
16
14
12
10
8
6
4
2
0
Xg (emu/g)
7x10⁴
6
5
4
3
2
1
0
1/Xg
0
40
80
120
160
200
240
280
320
TEMP. (°K)
Y Ni
GRAM SUSCEPTIBILITY VS TEMP.
@ 7200 GAUSS

Figure 3. Temperature and magnetic field dependence of the gram susceptibility of YNi_2. In the 7200 gauss curve, the dots and crosses represent experimental points obtained in different runs.

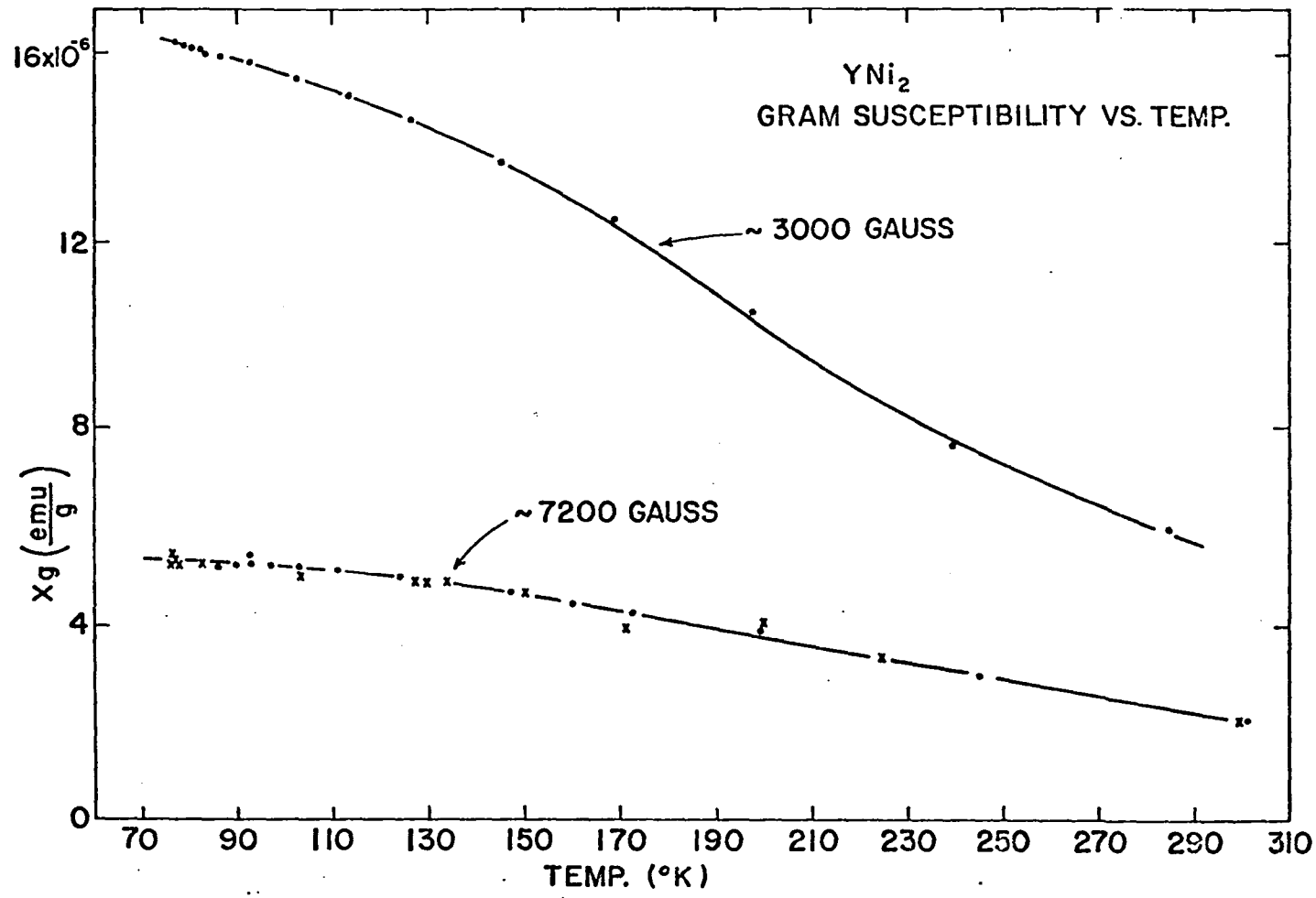
16x10⁻⁶
12
8
4
0
Xg (emu/g)
YNi2
GRAM SUSCEPTIBILITY VS. TEMP.
~ 3000 GAUSS
~ 7200 GAUSS
70
90
110
130
150
170
190
210
230
250
270
290
310
TEMP. (°K)

Figure 4. Temperature dependence of the gram susceptibility of YNi_3. The dashed portion of the curve is meant to indicate that, except for the dip, the two ends of the data curve are continuous.

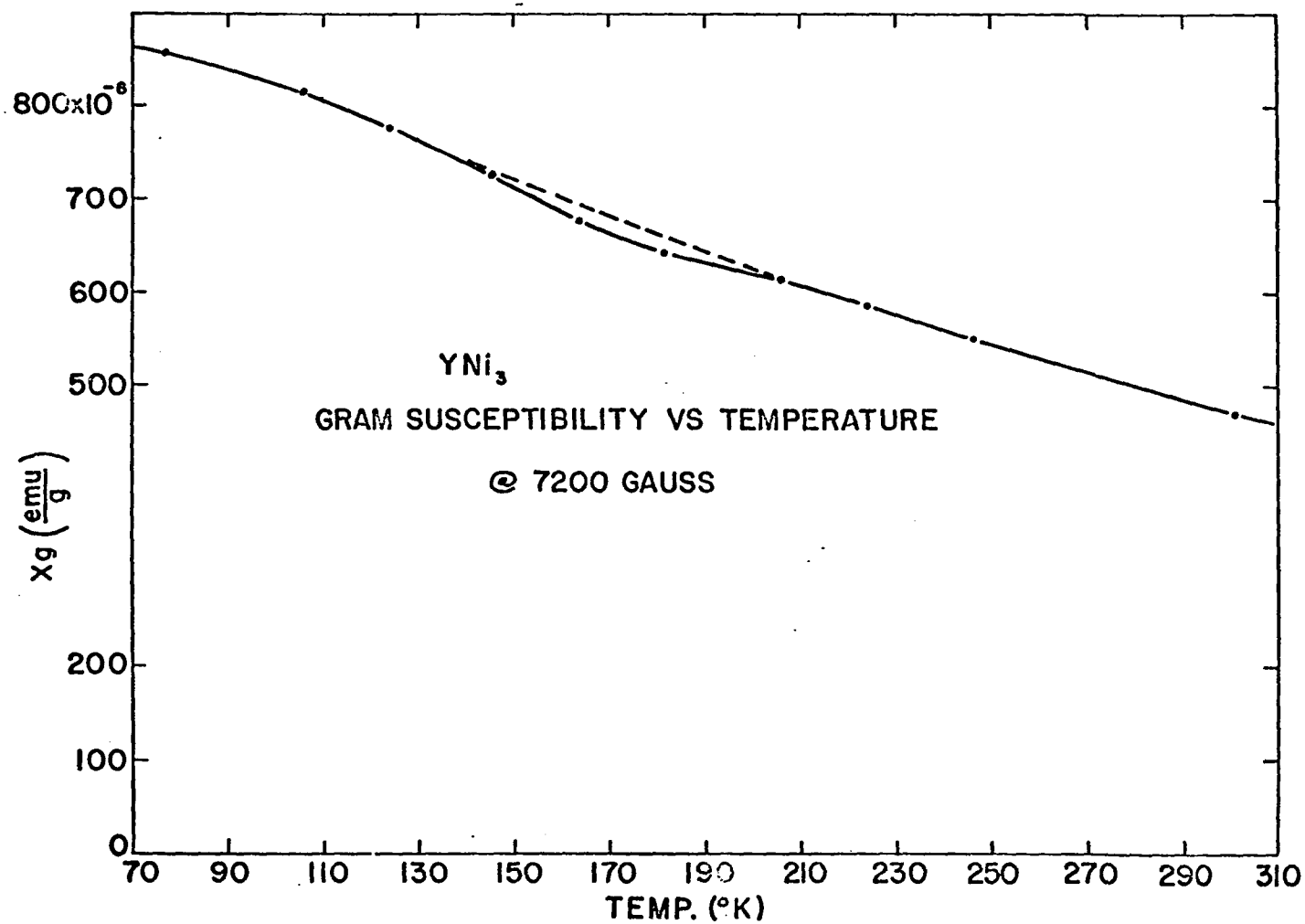
800x10⁻⁶
700
600
500
200
100
0
YNi₃
GRAM SUSCEPTIBILITY VS TEMPERATURE
@ 7200 GAUSS
Xg (emu/g)
70
90
110
130
150
170
190
210
230
250
270
290
310
TEMP. (°K)

Figure 5. Temperature dependence of the Y^{89} Knight shift in YMn_2. The error bars indicate the average deviation of the experimental value obtained.

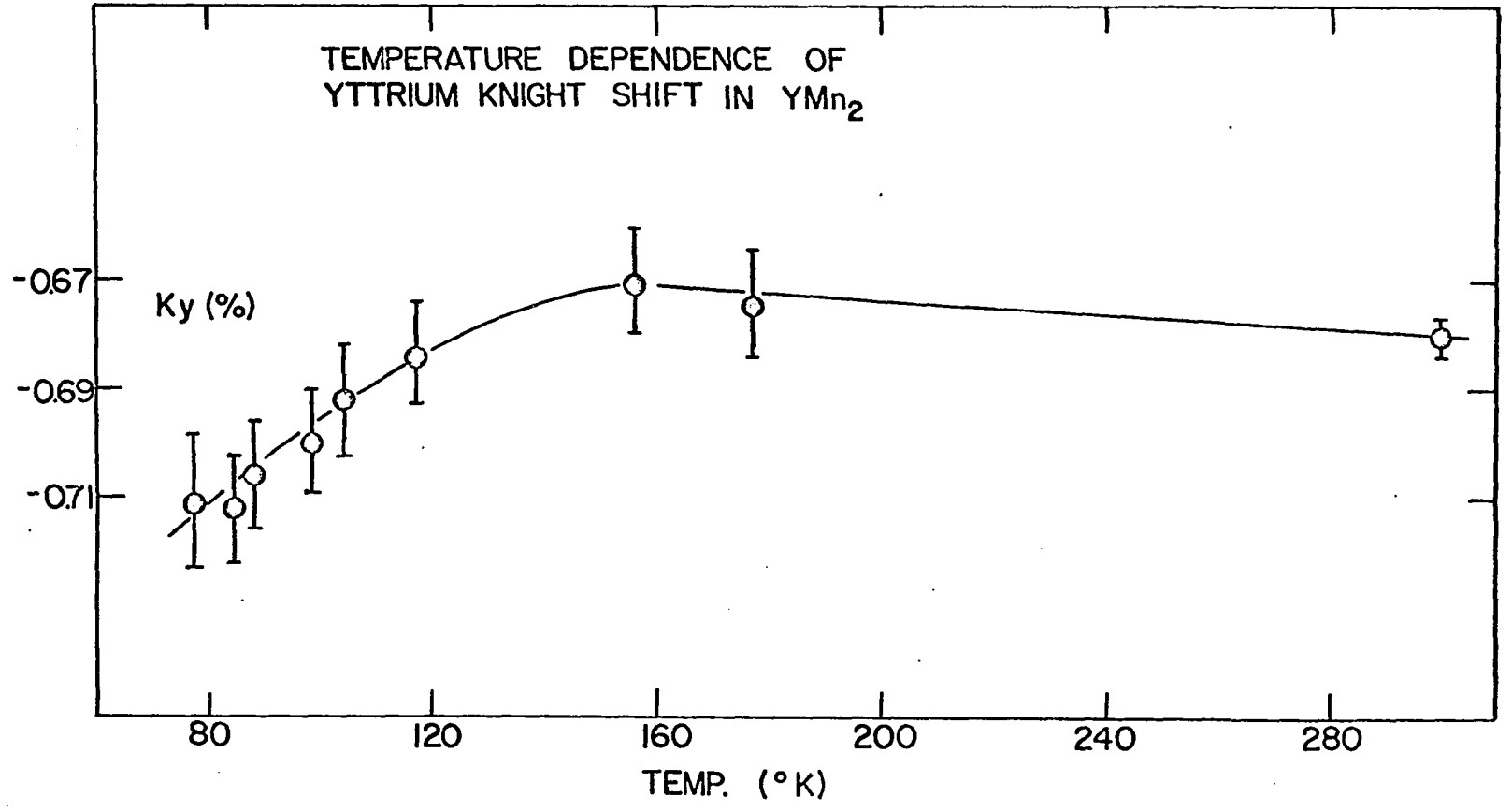
TEMPERATURE DEPENDENCE OF
YTTRIUM KNIGHT SHIFT IN YMn_2
Ky (%)
-0.67
-0.69
-0.71
80
120
160
200
240
280
TEMP. (°K)

Figure 6. Temperature and magnetic field dependence of the gram susceptibility of YMn_2. The dots and the crosses in the 6720 gauss curve represent different experimental runs.

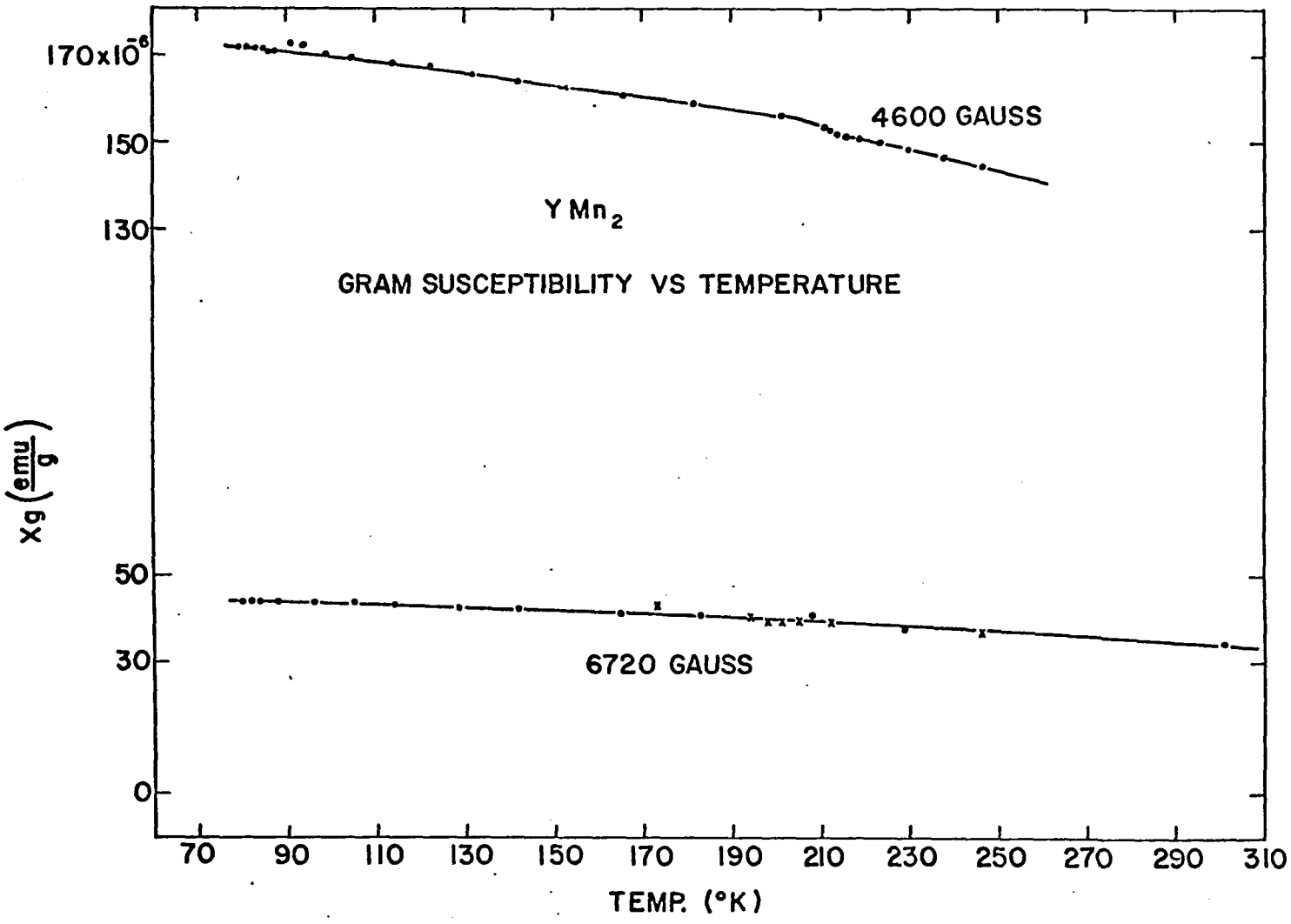
170x10⁻⁶
150
130
50
30
0
4600 GAUSS
YMn2
GRAM SUSCEPTIBILITY VS TEMPERATURE
6720 GAUSS
Xg (emu/g)
70
90
110
130
150
170
190
210
230
250
270
290
310
TEMP. (°K)

Figure 7. $\nu\Delta\nu$ vs. ν^2 for scandium metal at 77 ^{o}K and 300 ^{o}K. The arrows signify "correspond to".

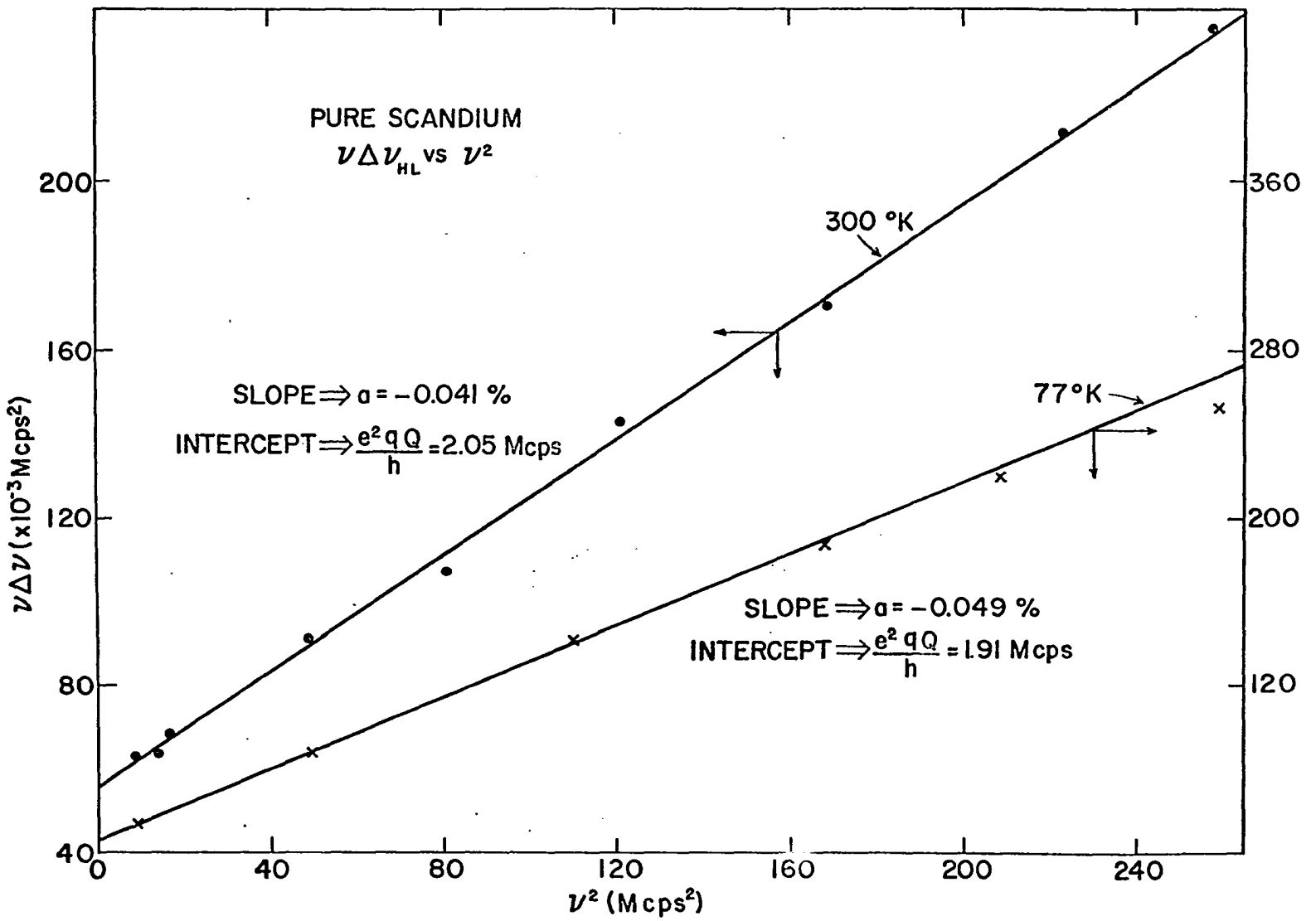
PURE SCANDIUM
$\nu\Delta\nu_{HL}$ vs ν^2
300 °K
77°K
SLOPE ⇒ a = −0.041 %
INTERCEPT ⇒ $\frac{e^2qQ}{h}$ = 2.05 Mcps
SLOPE ⇒ a = −0.049 %
INTERCEPT ⇒ $\frac{e^2qQ}{h}$ = 1.91 Mcps
$\nu\Delta\nu$ (x10^{-3}Mcps^2)
ν^2 (Mcps^2)
200
160
120
80
40
360
280
200
120
0
40
80
120
160
200
240

Figure 8. K_H and K_L vs. $1/\nu^2$ for scandium metal at 300 ^{o}K. The equations the lines represent are indicated on the figure.

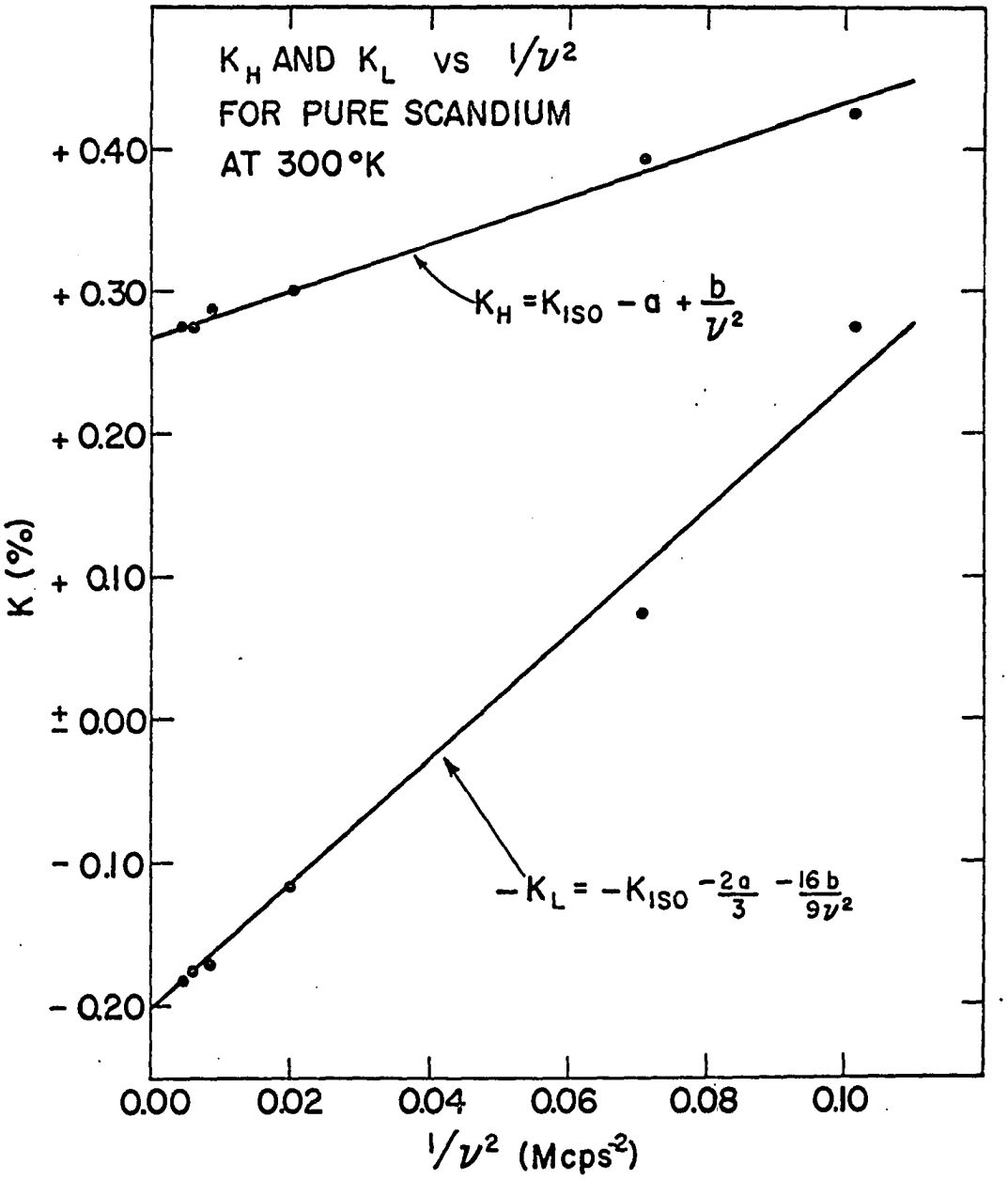
K_H AND K_L VS $1/\nu^2$
FOR PURE SCANDIUM
AT 300°K
$K_H = K_{ISO} - a + \frac{b}{\nu^2}$
$-K_L = -K_{ISO} - \frac{2a}{3} - \frac{16b}{9\nu^2}$
+ 0.40
+ 0.30
+ 0.20
+ 0.10
± 0.00
- 0.10
- 0.20
K (%)
0.00
0.02
0.04
0.06
0.08
0.10
$1/\nu^2$ (Mcps^{-2})

Figure 9. $\nu\Delta\nu$ vs. ν^2 for scandium nuclear magnetic resonance in scandium-yttrium alloys at 300 °K. The lines drawn are least-squares fit to the data point.

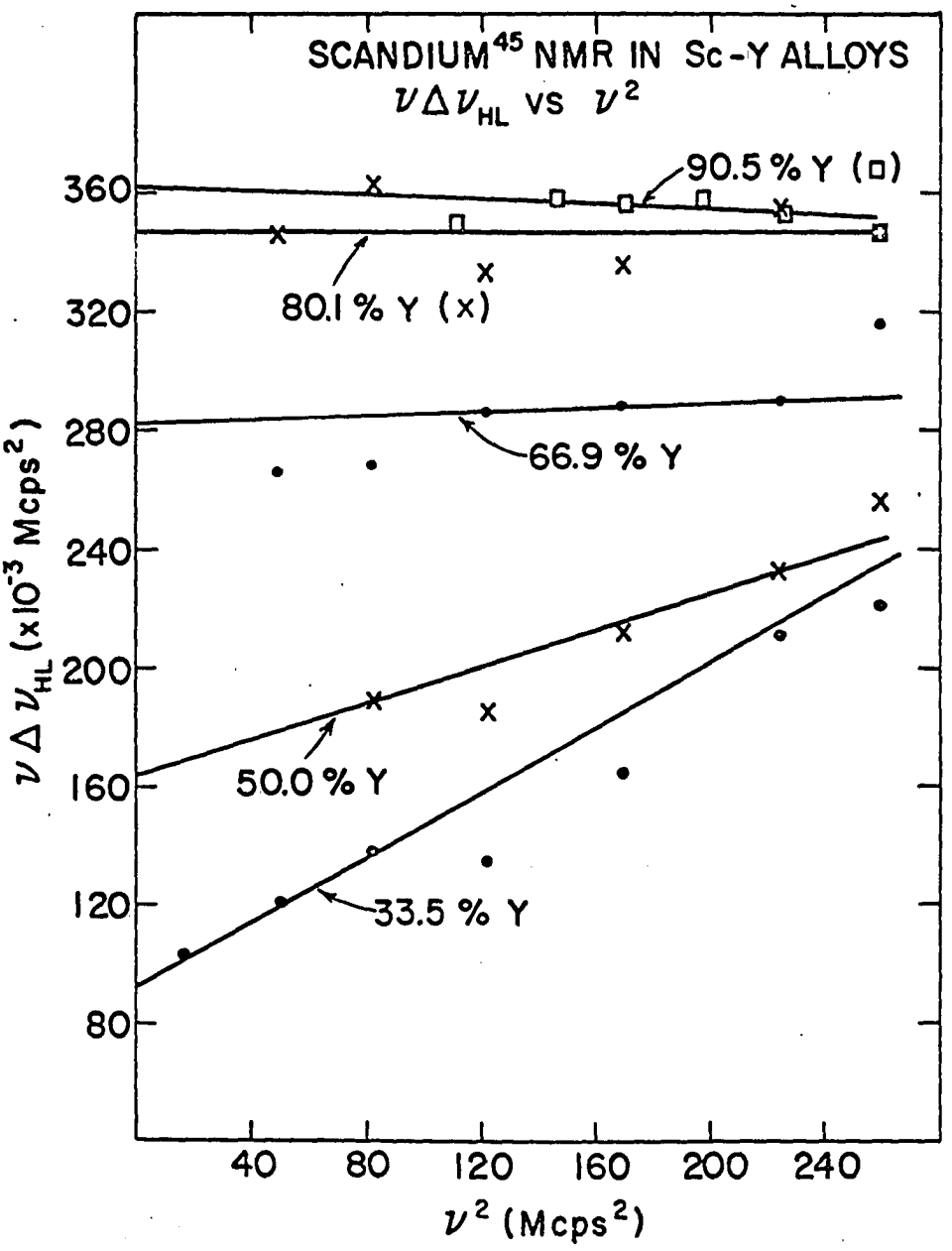
SCANDIUM 45 NMR IN Sc-Y ALLOYS
νΔν_HL VS ν²
90.5 % Y (□)
80.1 % Y (x)
66.9 % Y
50.0 % Y
33.5 % Y
νΔν_HL (x10⁻³ Mcps²)
ν² (Mcps²)
360
320
280
240
200
160
120
80
40
80
120
160
200
240

Figure 10. Experimental quadrupole coupling constants and anisotropic Knight shifts as a function of concentration in the scandium-yttrium system. The upper plot indicates the experimental quadrupole coupling constants and the theoretical lattice contribution is the solid line. The lower plot indicates the experimental values of the anisotropic Knight shift obtained from method A.

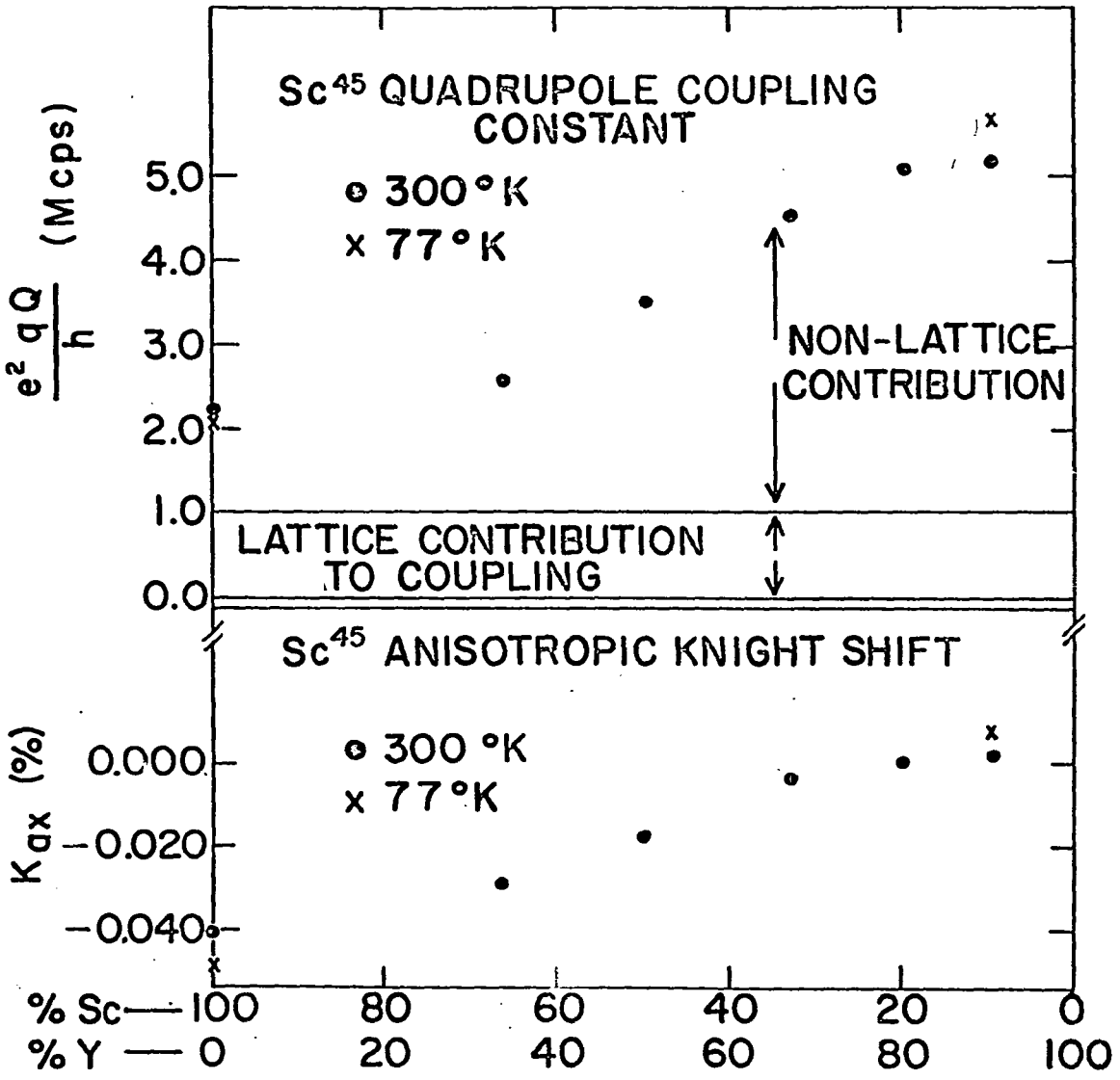
Sc45 QUADRUPOLE COUPLING CONSTANT
300 °K
77 °K
NON-LATTICE CONTRIBUTION
LATTICE CONTRIBUTION TO COUPLING
e²qQ/h (Mcps)
5.0
4.0
3.0
2.0
1.0
0.0
Sc45 ANISOTROPIC KNIGHT SHIFT
300 °K
77 °K
Kax (%)
0.000
−0.020
−0.040
% Sc — 100 80 60 40 20 0
% Y — 0 20 40 60 80 100

Figure 11. Plot of the experimental values of the anisotropic Knight shift vs. $\Delta^{1/2}$. Δ is defined in the text as the non-lattice contribution to the coupling constant obtained by subtracting the theoretical lattice contribution from the experimental quadrupole coupling constant.

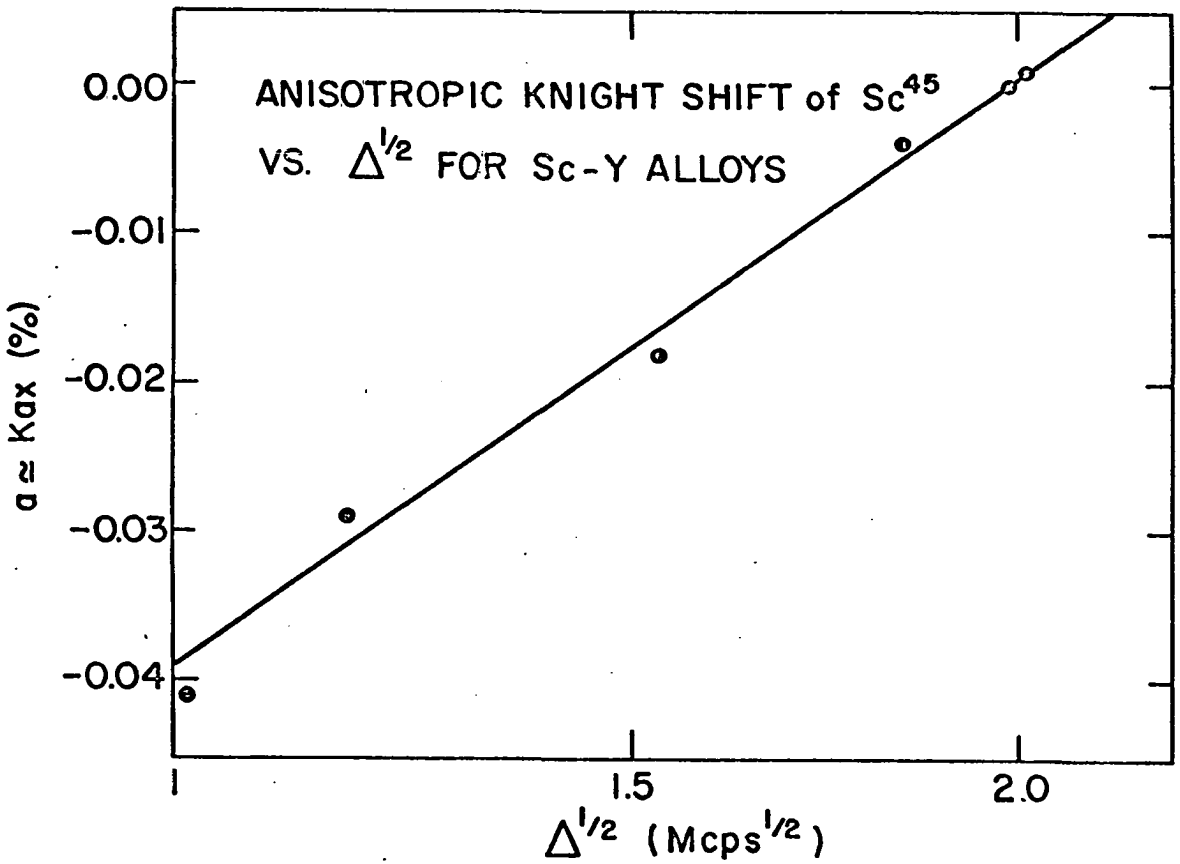
ANISOTROPIC KNIGHT SHIFT of Sc^{45}
VS. $\Delta^{1/2}$ FOR Sc-Y ALLOYS
0.00
-0.01
-0.02
-0.03
-0.04
a ≈ Kax (%)
1
1.5
2.0
$\Delta^{1/2}$ (Mcps$^{1/2}$)